

Laser spectroscopy to probe physics within and beyond the standard model

Simon Stellmer

Quantum Metrology Research Group

Particle Physics Seminar | 27.10.2022



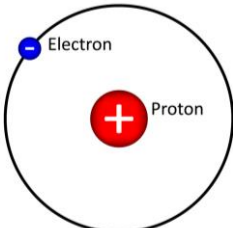
“Never measure anything but frequency!”

Arthur Schawlow

1. Electron-proton mass ratio $\mu = m_e/m_p$

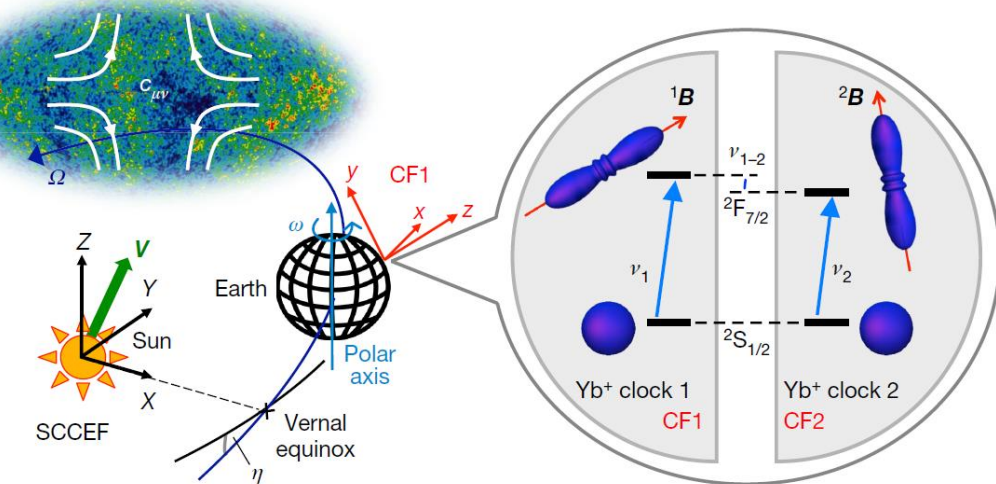
(by comparing the energy of various transitions over time)

$$\left(\frac{1}{\mu}\right) \left(\frac{d\mu}{dt}\right) = -0.5(1.6) \times 10^{-16} / \text{yr}$$



Phys. Rev. Lett. **113**, 210802 (2014)

2. Lorentz invariance



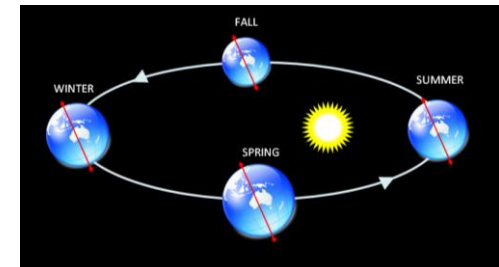
$$2.8 (4.2) \times 10^{-18}$$

Nature **567**, 204 (2019)

3. Local position invariance

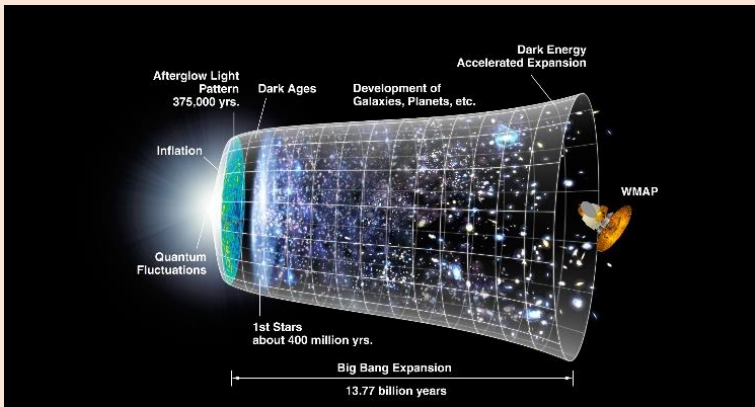
$$\left(\frac{c^2}{\alpha}\right) \left(\frac{d\alpha}{d\Phi}\right) = 14(11) \times 10^{-9}$$

Phys. Rev. Lett. **126**, 011102 (2021)

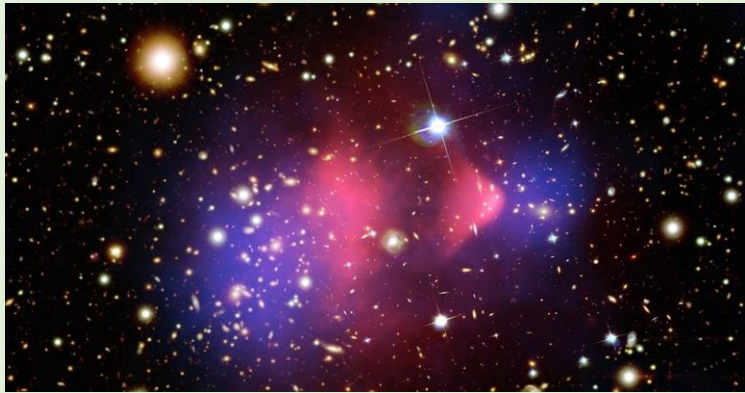


Grand challenges in fundamental physics

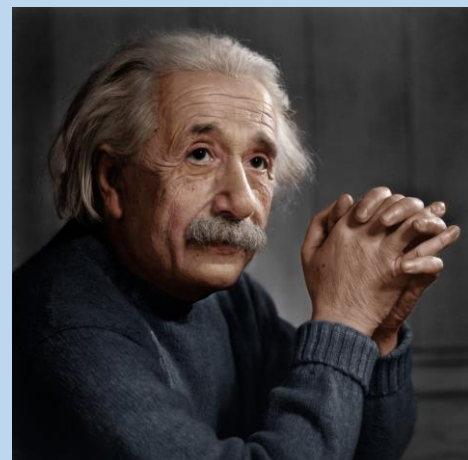
Baryon asymmetry



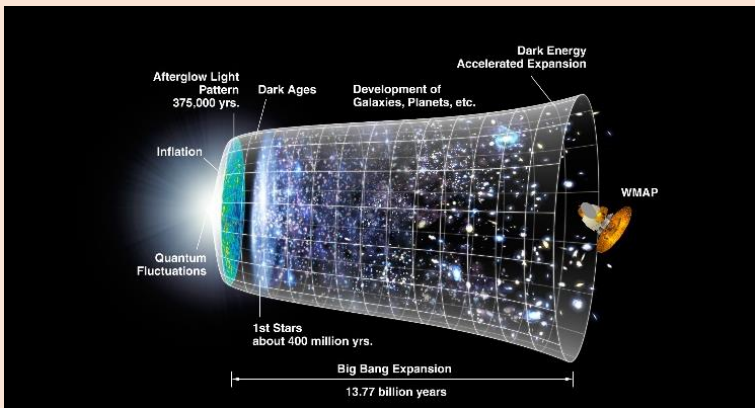
New particles



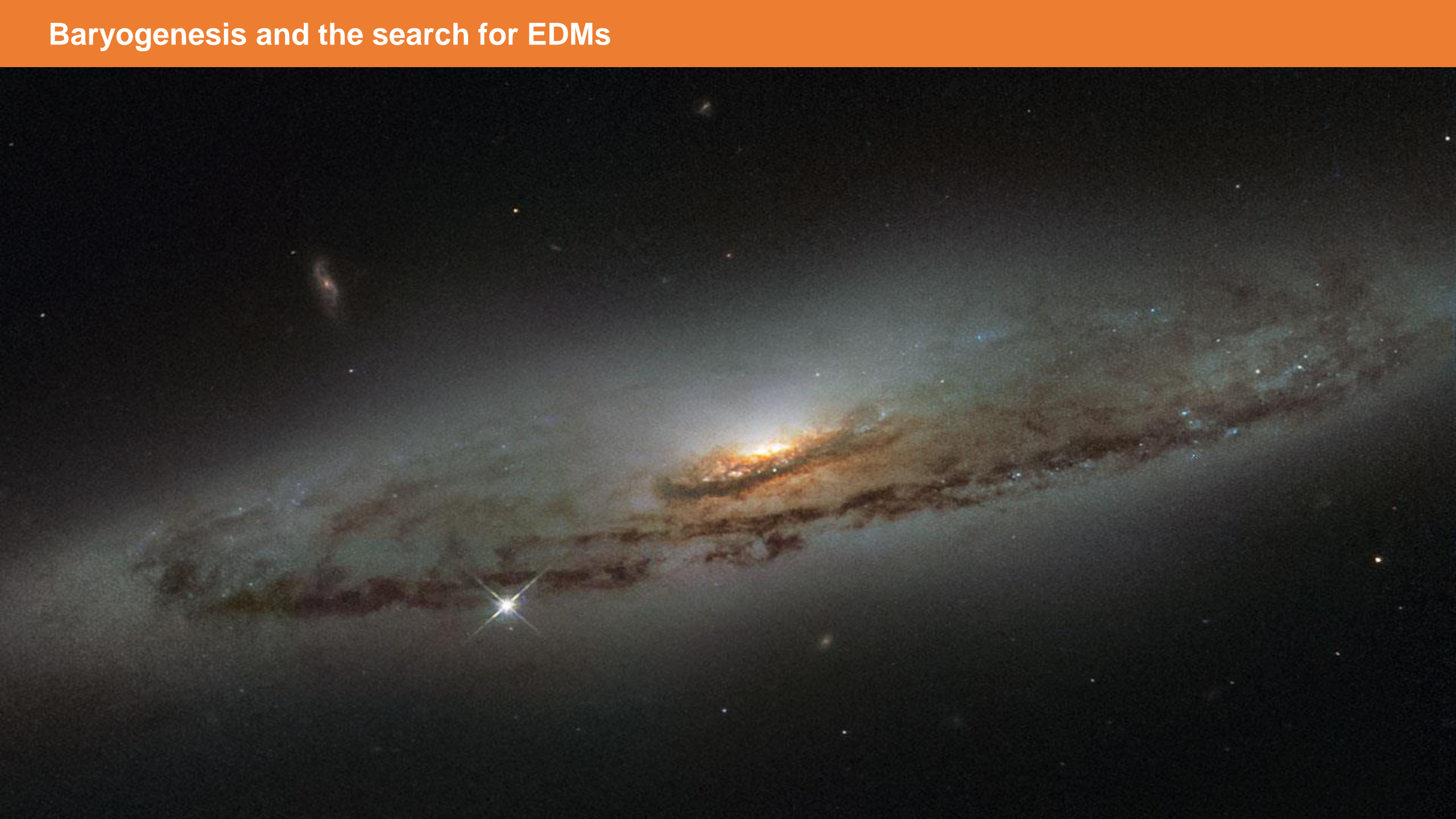
Test of special relativity



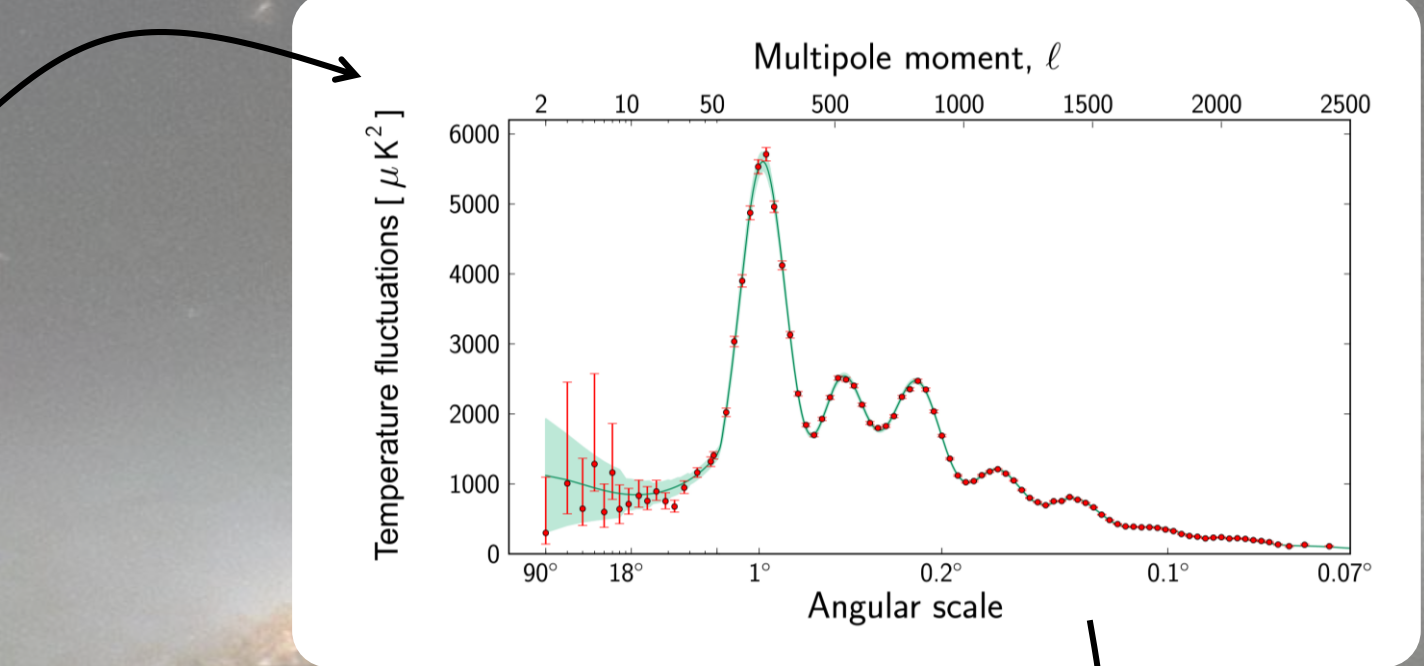
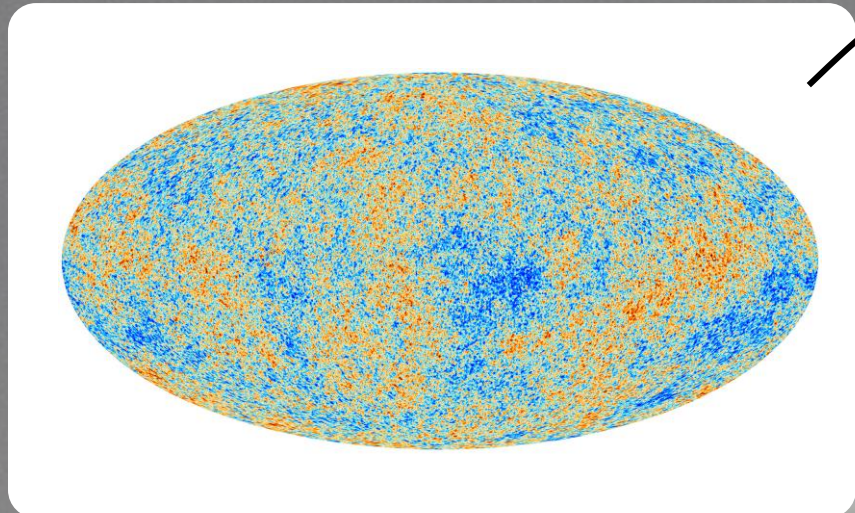
Baryon asymmetry



Baryogenesis and the search for EDMs



Baryogenesis and the search for EDMs



Baryon asymmetry:

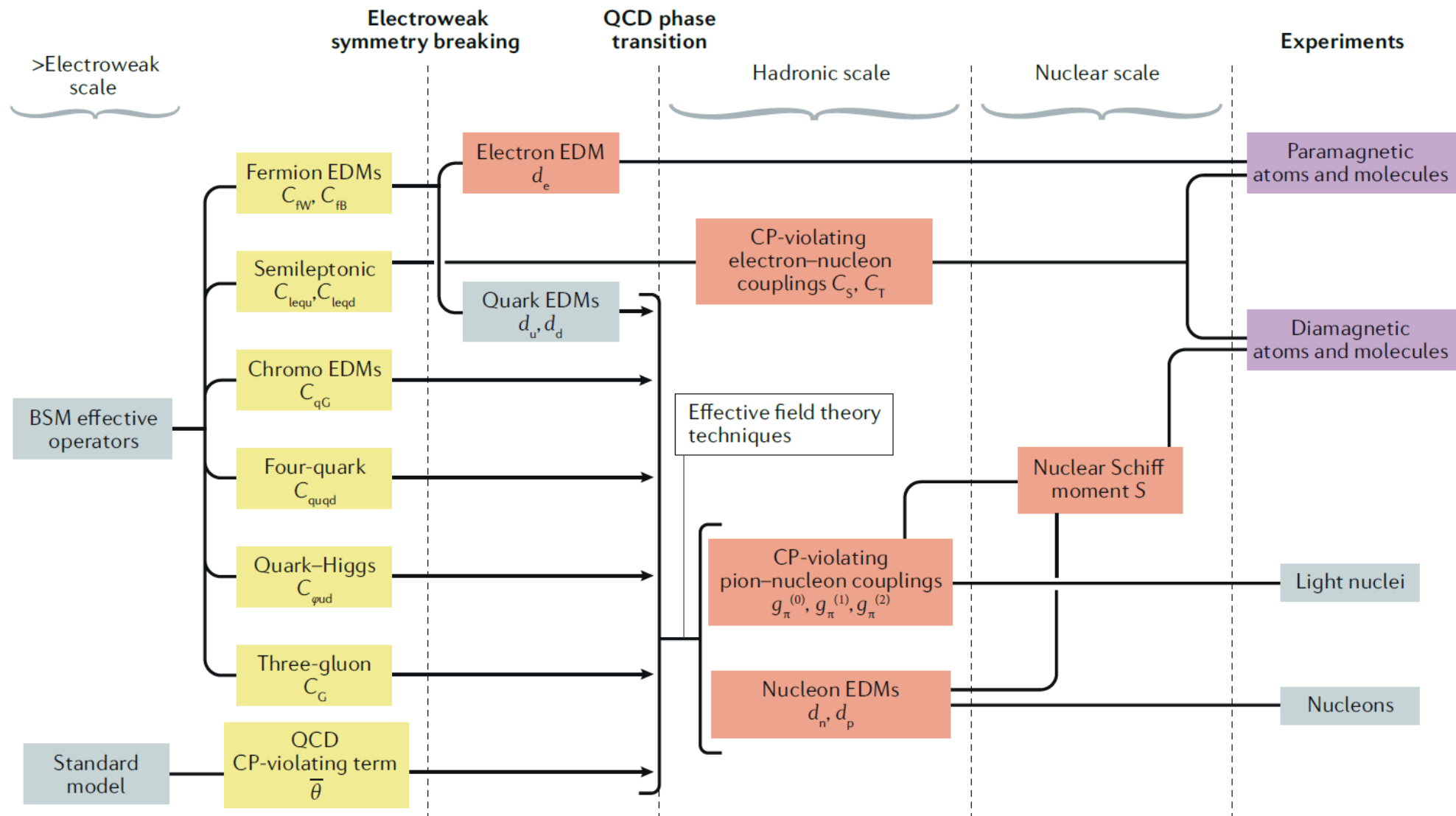
$$\eta = \frac{n_b - n_{\bar{b}}}{n_\gamma}$$

Standard model prediction: $\eta \sim 10^{-18}$

CMB measurements: $\eta = 6.11(30) \times 10^{-10}$

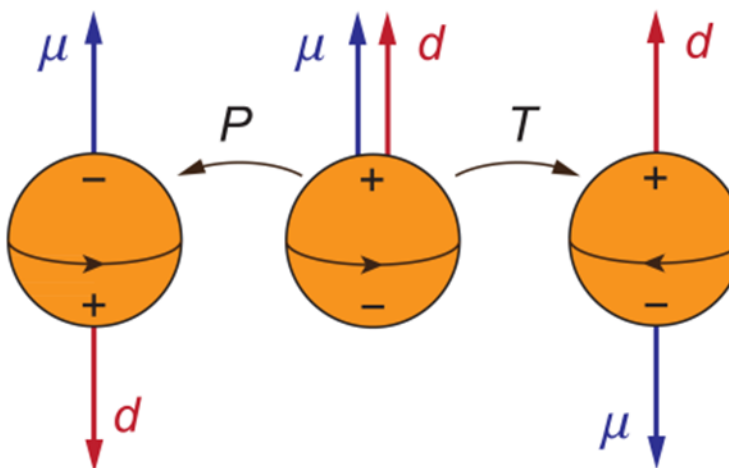
-> 8 orders of magnitude tension
-> 5% uncertainty on the measurement !!!

Baryogenesis and the search for EDMs



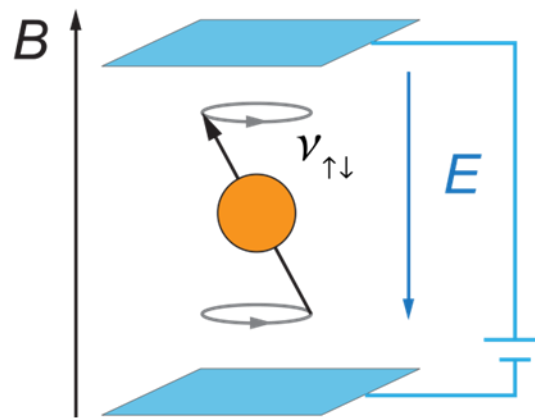
Baryogenesis and the search for EDMs

General idea:



T-violation is equivalent to CP-violation (because of CPT!)

General concept:



Larmor frequency:

$$h\nu = |2\mu B \pm 2dE|$$

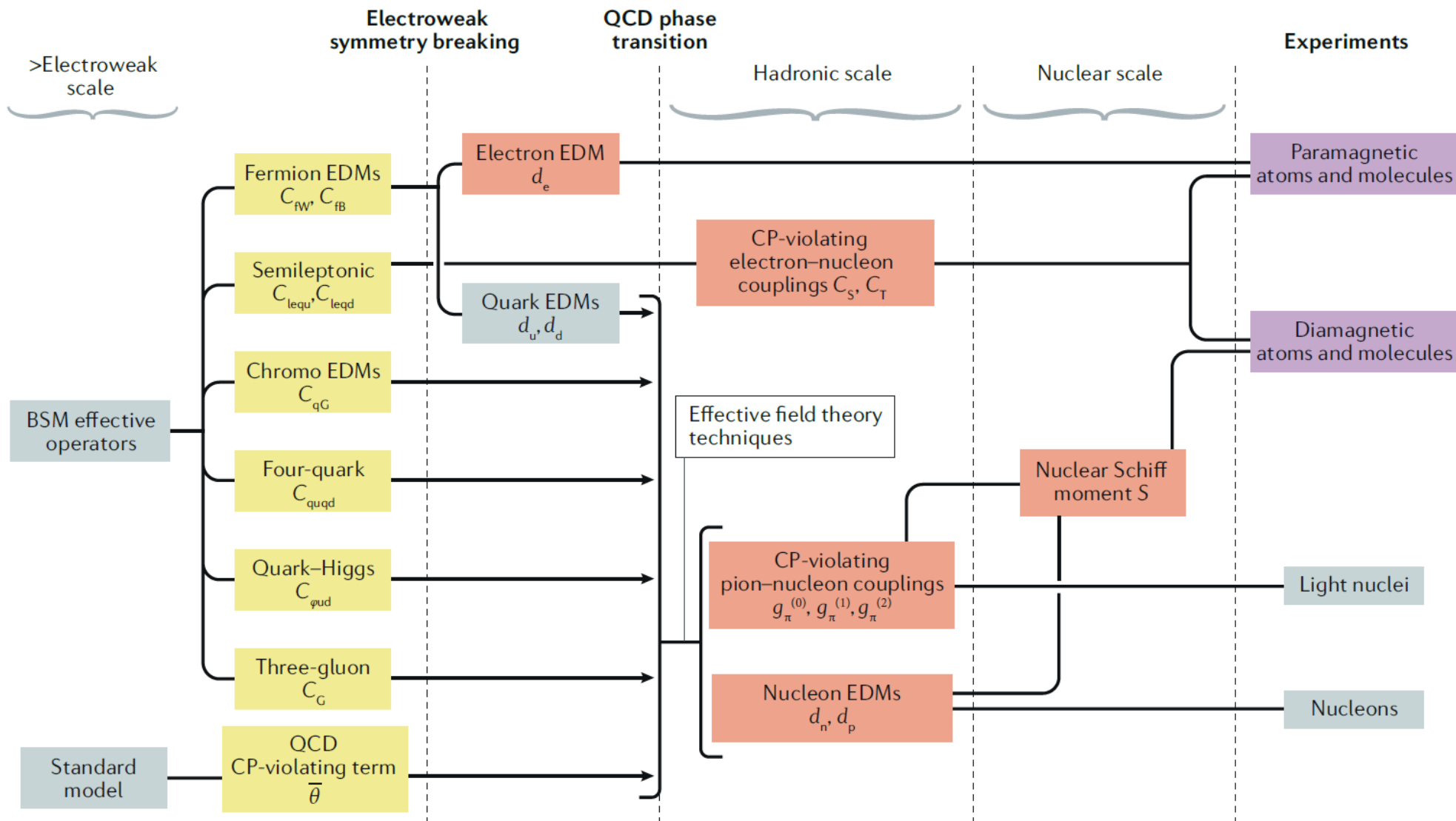
Dipole moment:

$$d = \frac{h \Delta\nu}{4E}$$

Sensitivity:

$$\delta d = \frac{\hbar}{2E \sqrt{2N\tau T}}$$

Baryogenesis and the search for EDMs



Baryogenesis and the search for EDMs

Electron EDM (e.g. Stanford, Imperial College, Harvard, JILA, ...)

ACME 2018 result: $d_e = (4.3 \pm 3.1_{stat} \pm 2.6_{syst}) \times 10^{-30} e \text{ cm}$
 $|d_e| < 1.1 \times 10^{-29} e \text{ cm}$

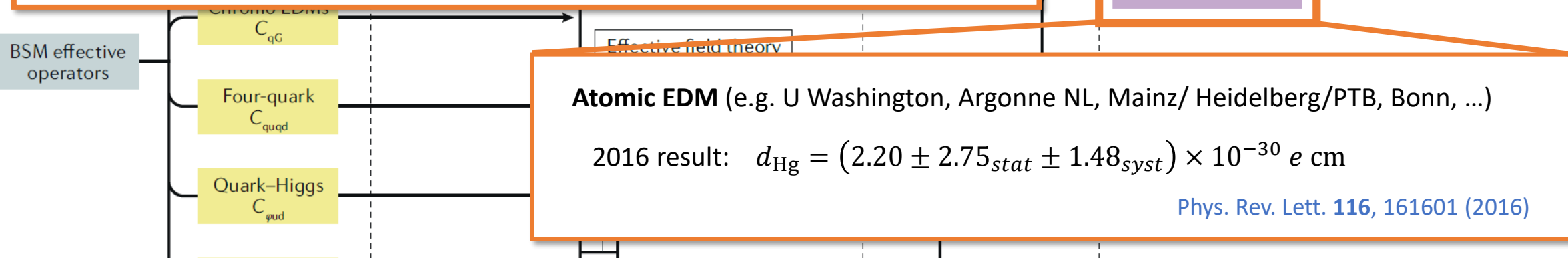
Nature 562, 355 (2018)

In typical models, where d_e is produced by one- or two-loop diagrams, for $\sin(\phi_T) \approx 1$ our result typically limits time-reversal-symmetry-violating new physics to energy scales above $\Lambda \approx 30 \text{ TeV}$ or $\Lambda \approx 3 \text{ TeV}$, respectively^{4–8}.

Experiments

Paramagnetic atoms and molecules

Diamagnetic atoms and molecules



Neutron EDM (e.g. Harvard, (...), ILL Grenoble, PSI, ...)

nEDM 2020 result: $d_n = (0.0 \pm 1.1_{stat} \pm 0.2_{syst}) \times 10^{-26} e \text{ cm}$
 $|d_n| < 1.8 \times 10^{-26} e \text{ cm}$

Phys. Rev. Lett. 124, 081803 (2020)

Nucleons

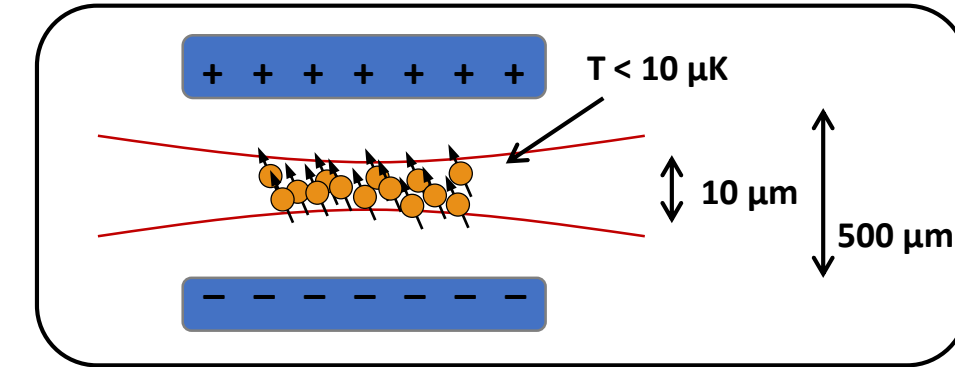
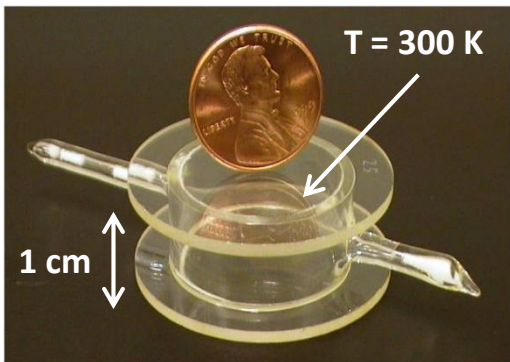
A new approach: ultracold atoms

$$EDM \sim Z^3$$

hydrogen 1 H 1.0079	beryllium 4 Be 9.0122	helium 2 He 4.0026
lithium 3 Li 6.941	magnesium 12 Mg 24.305	neon 10 Ne 20.180
sodium 11 Na 22.990	calcium 20 Ca 40.078	argon 18 Ar 39.948
potassium 19 K 39.098	strontium 38 Sr 87.62	krypton 36 Kr 83.80
rubidium 37 Rb 85.468	barium 56 Ba 132.91	xenon 54 Xe 131.29
caesium 55 Cs 132.91	lutetium 71 Lu 174.97	polonium 84 Po [210]
francium 87 Fr [223]	rutherfordium 102 Rf [261]	astatine 85 At [222]
radon 86 Ra [226]	lawrencium 103 Lr [262]	rhenium 75 Re 186.21
*	*	osmium 76 Os 190.23
89-102	89-102	iridium 77 Ir 192.22
*	*	platinum 78 Pt 195.08
		gold 79 Au 196.97
		mercury 80 Hg 200.59
		thallium 81 Tl 204.38
		lead 82 Pb 207.2
		bismuth 83 Bi 208.98
		polonium 84 Po [209]
		astatine 85 At [210]
		radon 86 Rn [222]
		freronium 103 Fl [289]
		moscovium 104 Mc [293]
		livermoreium 105 Lv [294]
		tennesseeium 106 Ts [294]
		oganesson 107 Og [294]

lanthanum 57 La 138.91	cerium 58 Ce 140.12	praseodymium 59 Pr 140.91	neodymium 60 Nd 144.24	promethium 61 Pm [145]	samarium 62 Sm 150.36	europerium 63 Eu 151.96	gadolinium 64 Gd 157.25	terbium 65 Tb 158.93	dysprosium 66 Dy 162.50	holmium 67 Ho 164.93	erbium 68 Er 167.26	thulium 69 Tm 168.93	yterbium 70 Yb 173.04
actinium 91 Ac [227]	thorium 90 Th 232.04	protactinium 91 Pa 231.04	uraniun 92 U 238.03	neptunium 93 Np [237]	plutonium 94 Pu [244]	amerium 95 Am [243]	curium 96 Cm [247]	berkelium 97 Bk [247]	californium 98 Cf [251]	einsteinium 99 Es [252]	fermiium 100 Fm [257]	mendelevium 101 Md [258]	nobelium 102 No [259]

A new approach: ultracold atoms



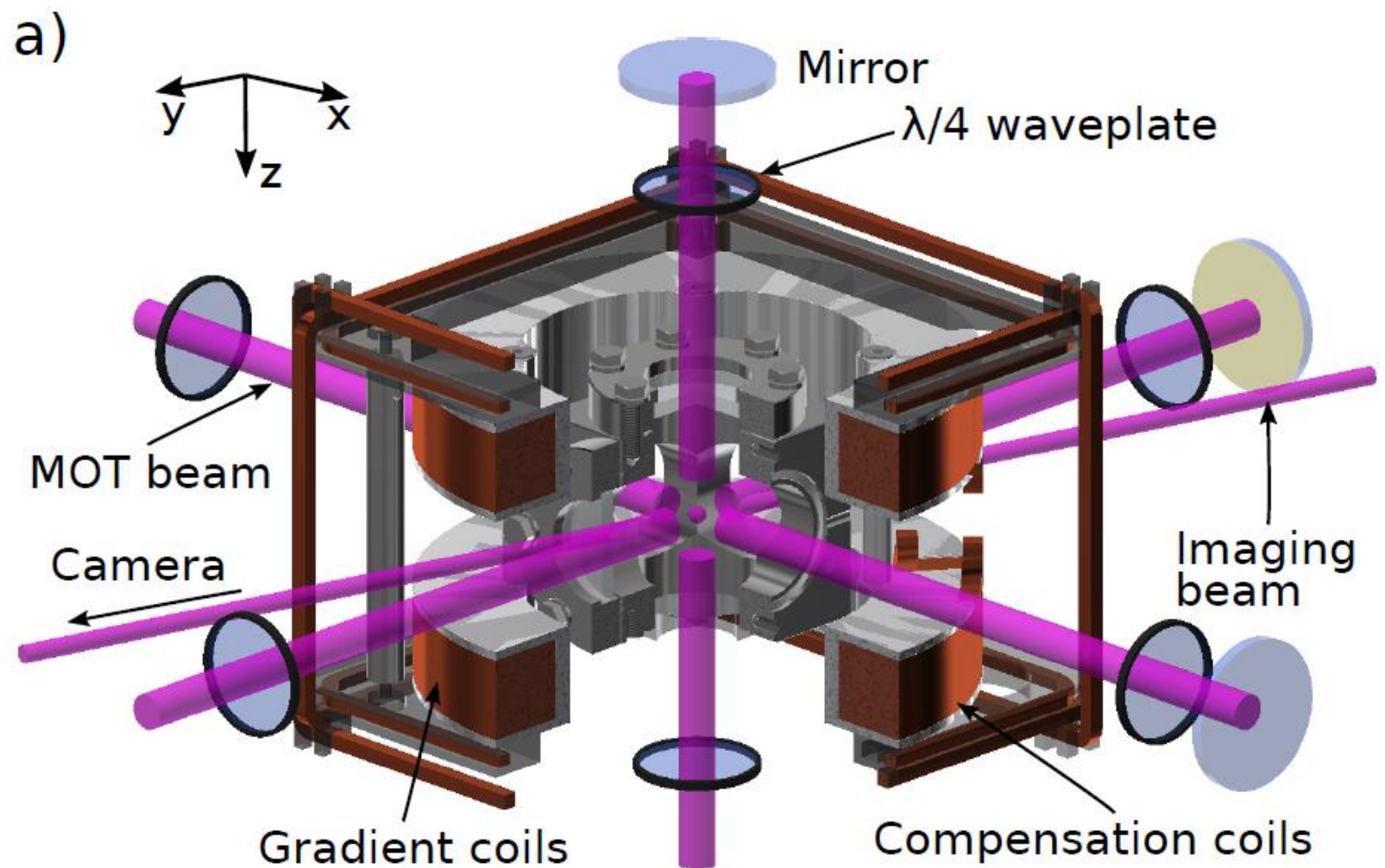
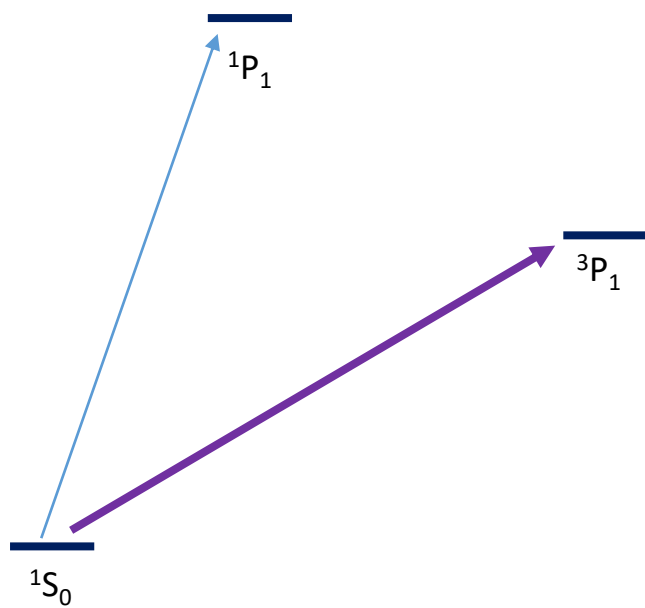
Sensitivity:

$$\delta d = \frac{\hbar}{2E \sqrt{2N\tau T}}$$

	Seattle (2016)	quMercury		
		conservative	optimistic	Heisenberg
voltage	15 kV	10 kV	30 kV	30 kV
electrode gap	1.1 cm	0.5 mm	0.5 mm	1 mm
E-field	13.6 kV/cm	200 kV/cm	600 kV/cm	300 kV/cm
spin decoherence τ	100 s	100 s	300 s	100 s
atom number N	2×10^{14}	10^6	10^8	10^7
measurement time T	10 months	3 months	3 months	3 months
design sensitivity δd	$(2 \times 10^{-33} e \text{ cm})$	$1.5 \times 10^{-28} e \text{ cm}$	$7.6 \times 10^{-31} e \text{ cm}$	$2.6 \times 10^{-33} e \text{ cm}$
experimental sensitivity δd	$7.4 \times 10^{-30} e \text{ cm}$			

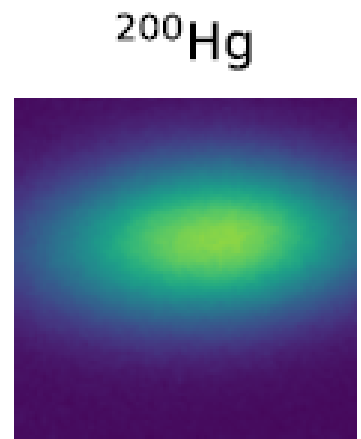
A new approach: ultracold atoms

254-nm laser system:
Toptica FHG,
200 – 300 mW

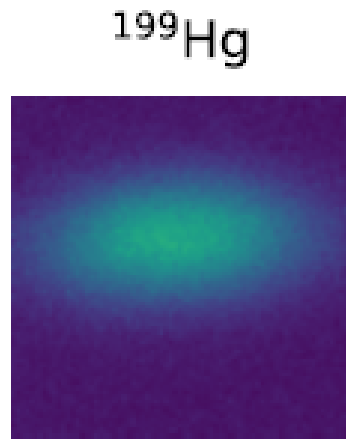


A new approach: ultracold atoms

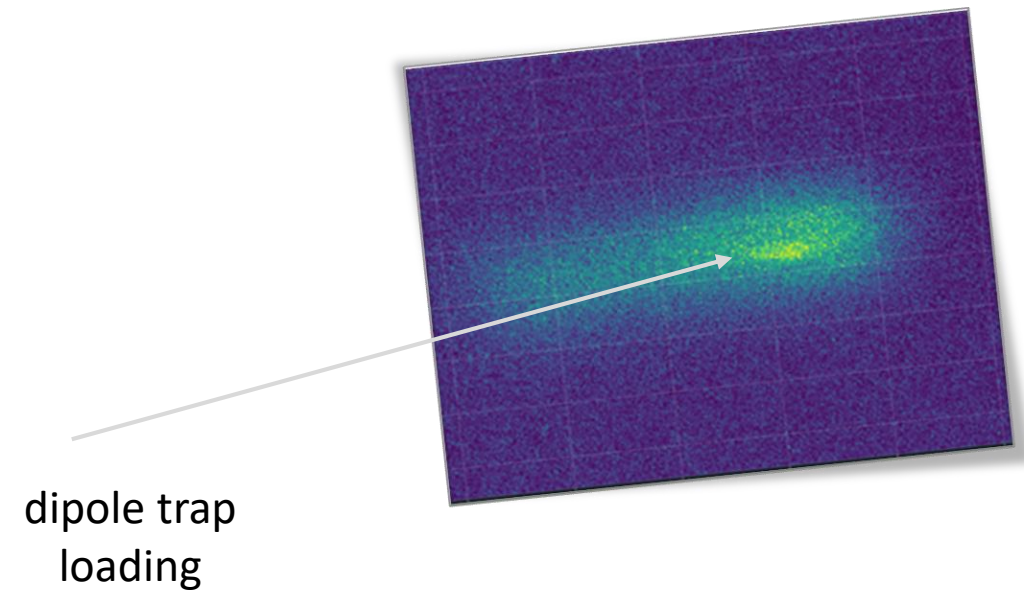
Magneto-optical trapping of mercury



10^8 atoms
200 μK temperature

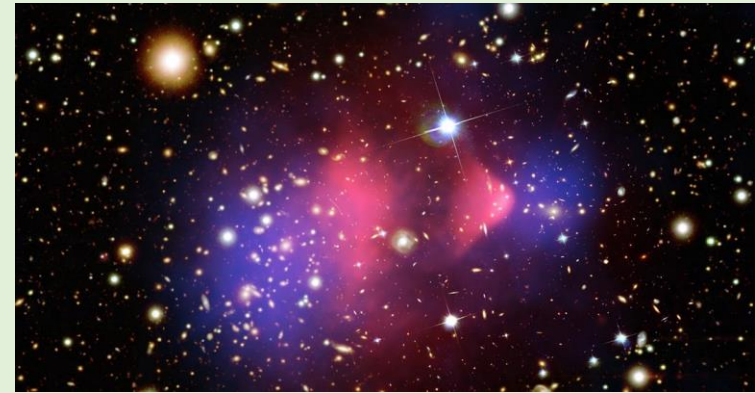


5×10^6 atoms
30 μK temperature



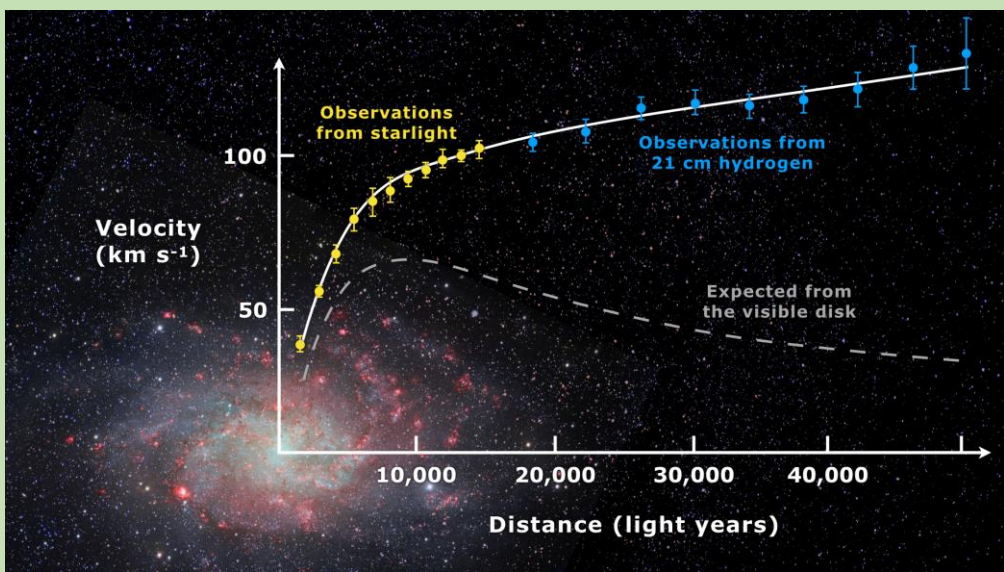
Next steps: optimization, scattering properties, evaporative cooling, quantum degeneracy, electric field plates, ...

Dark matter

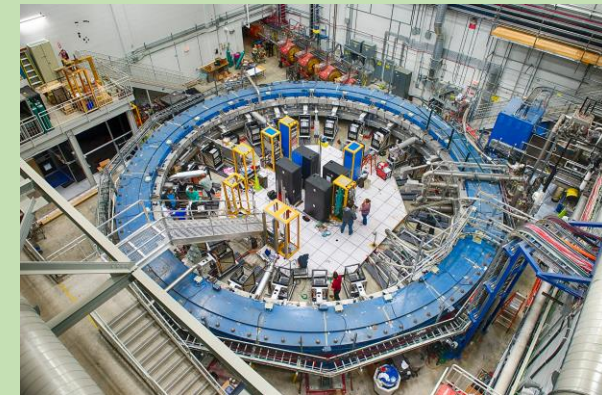


Search for new particles

Dark matter



Muon g-2



Fermilab (2021):

$$\frac{g - 2}{2} = 0,001\ 165\ 920\ 40\ (54)$$

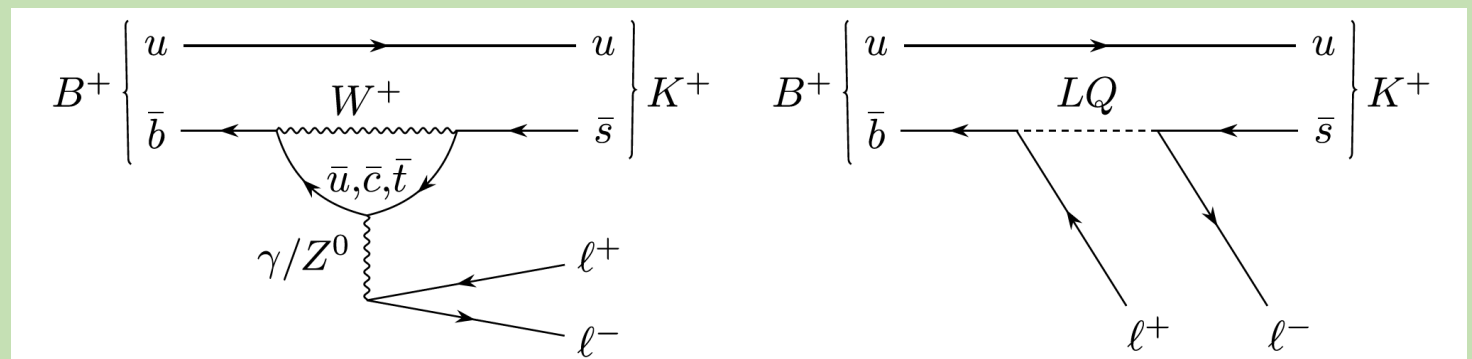
3.3 σ from SM calculations

Lepton universality

LHCb (2021):

$$B^+ \rightarrow K^+ \mu^+ \mu^-$$
$$B^+ \rightarrow K^+ e^+ e^-$$

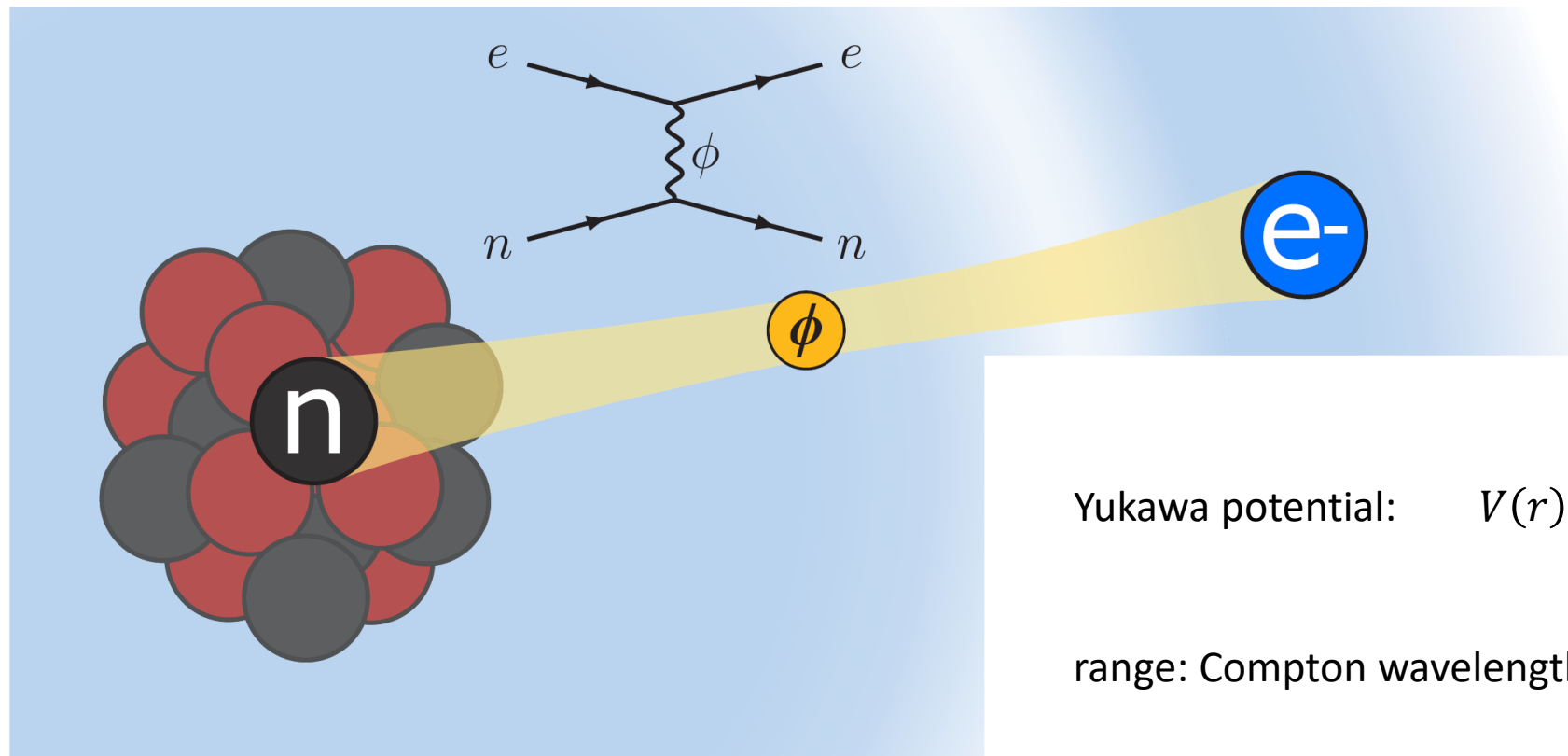
ratio: $R_K = 0.85(4)$



Isotope shift spectroscopy

Here:

Precision spectroscopy of optical transitions to search for a fifth force



Yukawa potential: $V(r) = \pm e^{-r/R} \frac{1}{R}$

range: Compton wavelength $R = \frac{\hbar}{mc}$

Experimental work:
MIT, Mainz, JQI, PTB, Stanford, Rice, Torun, Bonn, FHI, ...

Proposal: Phys. Rev. Lett. **120**, 091801 (2018)
MIT work: Phys. Rev. Lett. **125**, 123002 (2020)

Isotope shift spectroscopy

Isotope shift,

depends on **electronic orbital properties** + **nuclear properties**



$$\nu_{\alpha j i} =$$

isotopes i, j
transitions α, β

Isotope shift spectroscopy

Isotope shift,

depends on **electronic orbital properties** + **nuclear properties**



$$\nu_{\alpha ji} = F_\alpha \delta \langle r^2 \rangle_{ji}$$

field shift

(GHz scale)

isotopes i, j
transitions α, β

Isotope shift spectroscopy

Isotope shift,

depends on **electronic orbital properties** + **nuclear properties**



$$\nu_{\alpha ji} = F_\alpha \delta \langle r^2 \rangle_{ji} + K_\alpha \mu_{ji}$$

field shift

mass shift

(GHz scale)

(MHz scale)

isotopes i, j
transitions α, β

Isotope shift spectroscopy

Isotope shift,

depends on **electronic orbital properties** + **nuclear properties**



$$\nu_{\alpha ji} = F_\alpha \delta \langle r^2 \rangle_{ji} + K_\alpha \mu_{ji} + G_\alpha (\delta \langle r^2 \rangle_{ji})^2$$

field shift

(GHz scale)

mass shift

(MHz scale)

second-order

field shift

(kHz scale)

isotopes i, j
transitions α, β

Isotope shift spectroscopy

Isotope shift,

depends on **electronic orbital properties** + **nuclear properties** + **new physics**



$$\nu_{\alpha ji} = F_\alpha \delta\langle r^2 \rangle_{ji} + K_\alpha \mu_{ji} + G_\alpha (\delta\langle r^2 \rangle_{ji})^2 + v_{ne} D_\alpha a_{ji}$$

	<i>field shift</i> (GHz scale)	<i>mass shift</i> (MHz scale)	<i>second-order field shift</i> (kHz scale)	<i>New Boson</i> (Hz - kHz scale)
isotopes i, j transitions α, β				

Then:

1. Normalize by the mass shift μ_{ij}
2. Use a second optical transition β to remove the $\delta\langle r^2 \rangle_{ji}/\mu_{ij}$ field shift term

Isotope shift spectroscopy

Isotope shift
relation between depends on **electronic orbital properties** + **nuclear properties** + **new physics**
two optical transitions,

The diagram illustrates the components of isotope shift in a King plot. It shows the equation for the isotope shift $\tilde{\nu}_{\beta ji}$ as a sum of four terms: field shift, mass shift, second-order field shift, and New Boson. The first three terms are grouped under a bracket labeled 'linear' and 'offset', while the last term is labeled 'nonlinear'. The components are also associated with specific scales: GHz scale for field shift, MHz scale for mass shift, kHz scale for second-order field shift, and Hz - kHz scale for New Boson. The overall equation is:

$$\tilde{\nu}_{\beta ji} = F_{\beta\alpha} \tilde{\nu}_{\alpha ji} + K_{\beta\alpha} + G_{\beta\alpha} \left(\delta \langle r^2 \rangle_{ji} \right)^2 + v_{ne} D_{\beta\alpha} \tilde{a}_{ji}$$

isotopes i, j
transitions α, β

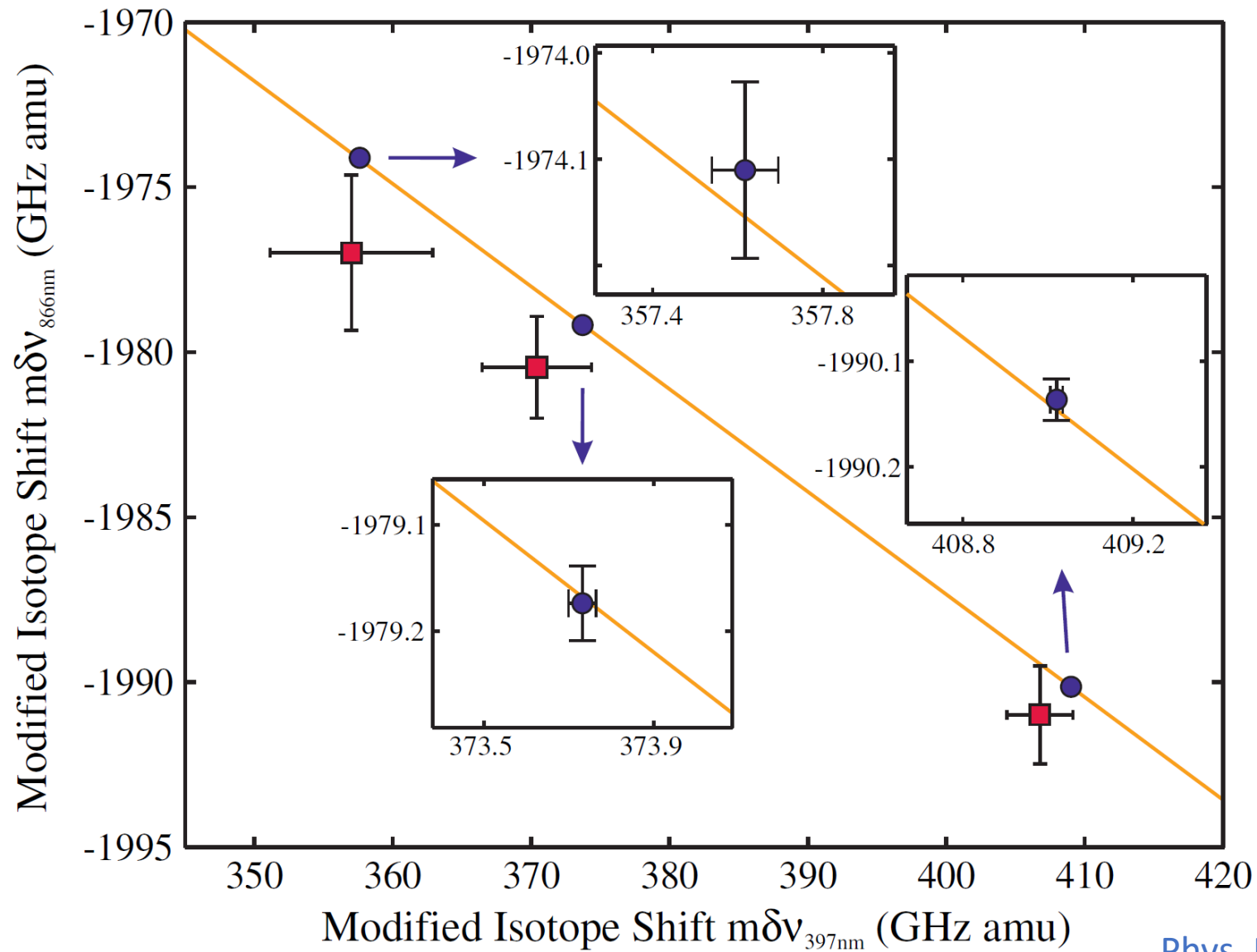
field shift (GHz scale) mass shift (MHz scale) second-order field shift (kHz scale) New Boson (Hz - kHz scale)

linear offset nonlinear / quadratic nonlinear

-> graphical representation: King plot

Isotope shift spectroscopy

A random example: Calcium ions



Isotope shift spectroscopy

Desiderata:

- element that can be laser-cooled & trapped
 - could be atoms or ions (also HClIs)
- as many isotopes as possible
 - stable
 - large spread of neutron numbers
- $I = 0$ to steer clear of hyperfine structure
- as many optical transitions as possible
 - the narrower, the better
 - connecting different orbitals

The image shows a standard periodic table of elements. A green rectangular box highlights a cluster of elements in the middle-right section: Calcium (Ca), Barium (Ba), Zinc (Zn), Cadmium (Cd), Mercury (Hg), and Ytterbium (Yb). These elements are chosen because they meet the criteria for isotope shift spectroscopy: they are stable, have multiple isotopes, and have nuclear spin I=0.

hydrogen 1 H 1.0079	lithium 3 Li 6.941	beryllium 4 Be 9.0122	magnesium 12 Mg 24.305	aluminum 13 Al 26.982	carbon 6 C 12.011	nitrogen 7 N 14.007	oxygen 8 O 15.999	fluorine 9 F 18.998	neon 10 Ne 20.180											
sodium 11 Na 22.990	potassium 19 K 39.098	calcium 20 Ca 40.078	strontium 38 Sr 87.62	yttrium 39 Y 88.906	titanium 22 Ti 47.867	vanadium 23 V 50.942	chromium 24 Cr 51.996	manganese 25 Mn 54.938	iron 26 Fe 55.845	cobalt 27 Co 58.933	nickel 28 Ni 58.693	copper 29 Cu 63.546	zinc 30 Zn 65.39	boron 5 B 10.811	silicon 14 Si 28.086	phosphorus 15 P 30.974	sulfur 16 S 32.065	chlorine 17 Cl 35.453	argon 18 Ar 39.948	
rubidium 37 Rb 85.468	cesium 55 Cs 132.91	barium 56 Ba 137.33	strontium 38 Sr 87.62	lutetium 57-70 * Lr 174.97	yttrium 39 Y 88.906	zirconium 40 Zr 91.224	niobium 41 Nb 92.906	chromium 24 Cr 95.94	technetium 43 Tc [98]	ruthenium 44 Ru 101.07	rhodium 45 Rh 102.91	palladium 46 Pd 106.42	silver 47 Ag 107.87	cadmium 48 Cd 112.41	indium 49 In 114.82	tin 50 Sn 118.71	antimony 51 Ge 121.76	selenium 34 As 126.90	bromine 35 Br 79.904	krypton 36 Kr 83.80
francium 8 Fr [223]	radium 8 Ra [226]	radioactive 89-102 * Rf [261]	lawrencium 10 Lr [262]	lanthanum 57 La 136.91	cerium 58 Ce 140.12	praseodymium 59 Pr 140.91	neodymium 60 Nd 144.24	promethium 61 Pm [145]	samarium 62 Sm 150.36	europeum 63 Eu 151.96	gadolinium 64 Gd 157.25	terbium 65 Tb 158.93	dysprosium 66 Dy 162.50	holmium 67 Ho 164.93	erbium 68 Er 167.26	thulium 69 Tm 168.93	yterbium 70 Yb 173.04			
radioactive 89-102 * Rf [261]	radioactive 9 Pa [231.04]	protactinium 9 U [238.03]	neptunium 9 Np [237]	plutonium 9 Pu [244]	americium 10 Am [243]	curium 10 Cm [247]	bcurium 10 Bk [247]	berkelium 10 Cf [251]	californium 10 Es [252]	einsteiniun 10 Fm [257]	mercury 10 Md [258]	radioactive 10 No [259]								

→ Ca, Ba, Zn, Cd, Hg, & Yb

Isotope shift spectroscopy

$$\tilde{\nu}_{\beta ji} = F_{\beta\alpha} \tilde{\nu}_{\alpha ji} + K_{\beta\alpha} + G_{\beta\alpha} (\delta \langle r^2 \rangle_{ji})^2 + v_{ne} D_{\beta\alpha} \tilde{a}_{ji}$$

field shift *mass shift* *second-order field shift* *New Boson*

linear offset nonlinear / quadratic nonlinear

Checklist:

- N isotopes (at least 4)
- N-1 differences between isotopes (at least 3)
- N-2 optical transitions (at least 2 for a 2D King plot)
- 1 „DOF“ used up for the mass shift („mass of nucleus“)
- 1 „DOF“ used up for the field shift („size of nucleus“)

-> 1 „DOF“ left for nonlinear terms

Isotope shift spectroscopy

$$\tilde{\nu}_{\beta ji} = F_{\beta\alpha} \tilde{\nu}_{\alpha ji} + K_{\beta\alpha} + G_{\beta\alpha} (\delta \langle r^2 \rangle_{ji})^2 + v_{ne} D_{\beta\alpha} \tilde{a}_{ji}$$

field shift *mass shift* *second-order field shift* *New Boson*

linear offset nonlinear / quadratic nonlinear

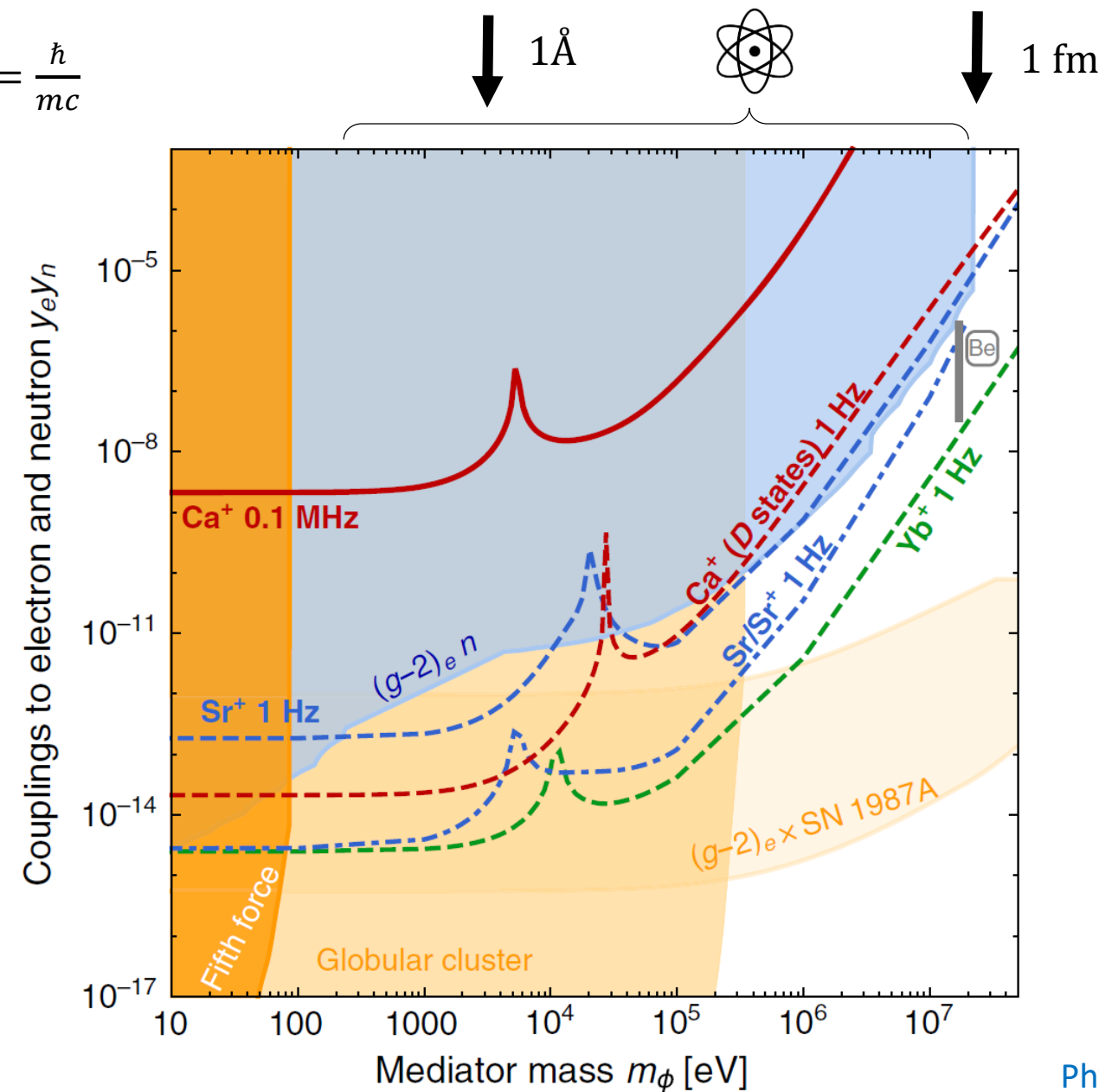
Checklist:

- N isotopes (**at least 5**)
- N-1 differences between isotopes (**at least 4**)
- N-2 optical transitions (**at least 3 for a 3D King plot**)
- 1 „DOF“ used up for the mass shift („mass of nucleus“)
- 1 „DOF“ used up for the field shift („size of nucleus“)
- 1 „DOF“ used up for the second-order field shift

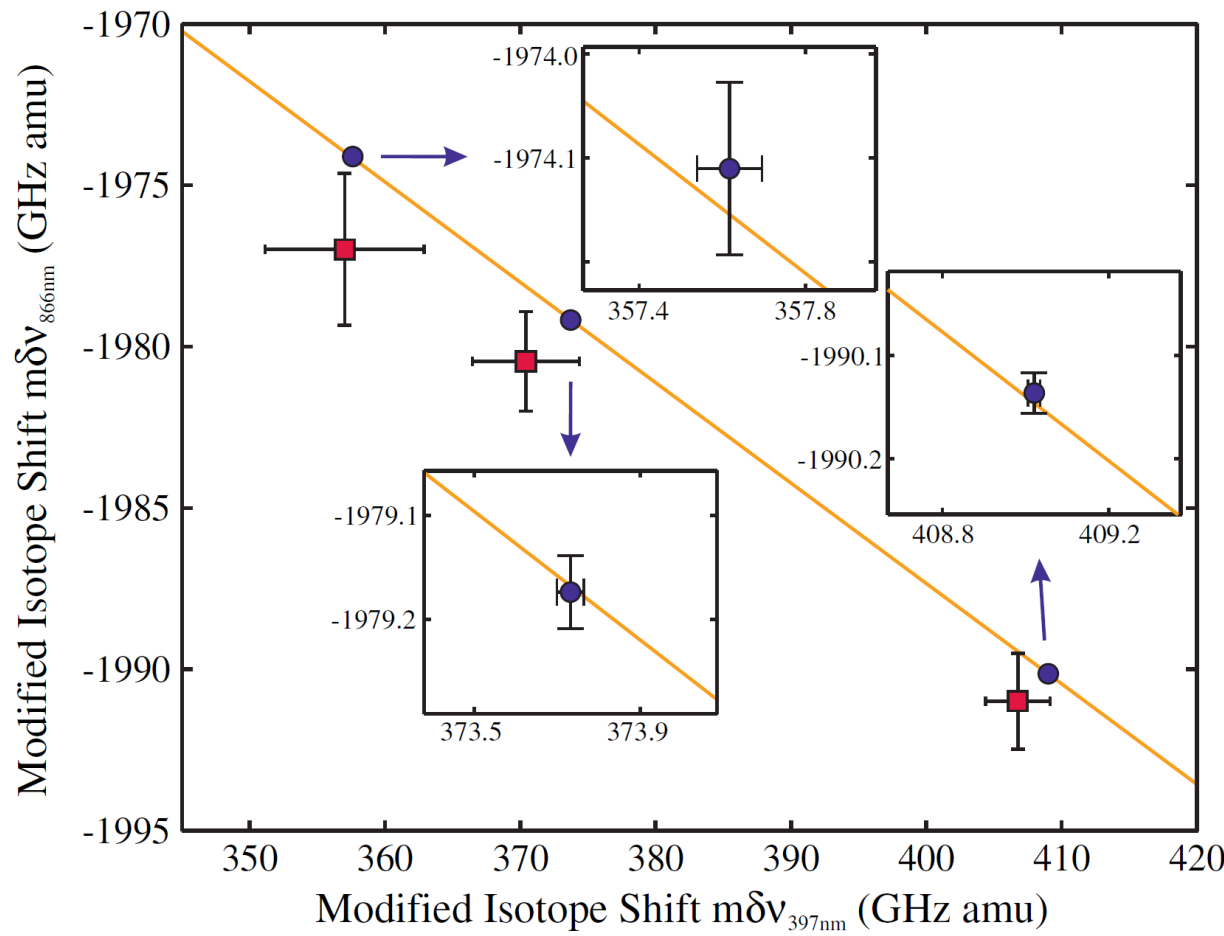
-> 1 „DOF“ left for nonlinear terms

Isotope shift spectroscopy

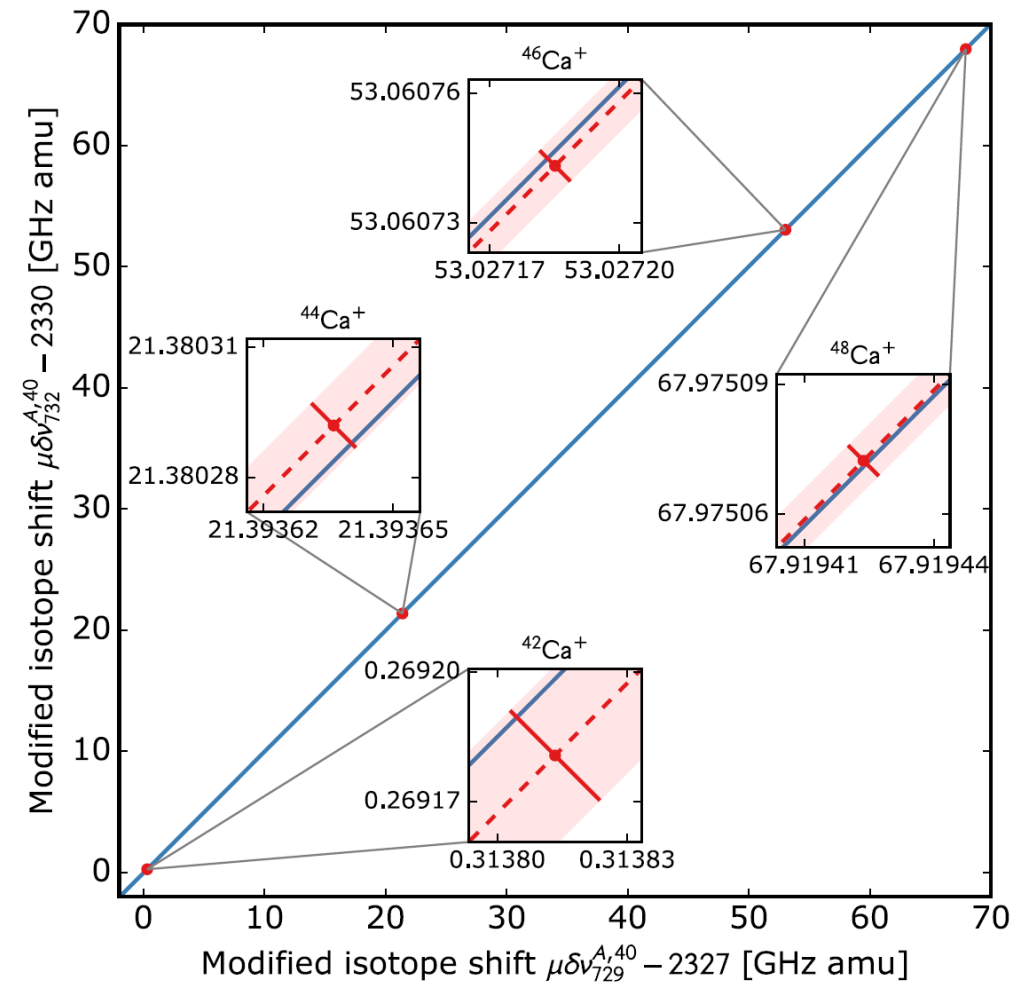
$$\text{range: } R = \frac{\hbar}{mc}$$



Isotope shift spectroscopy: Calcium

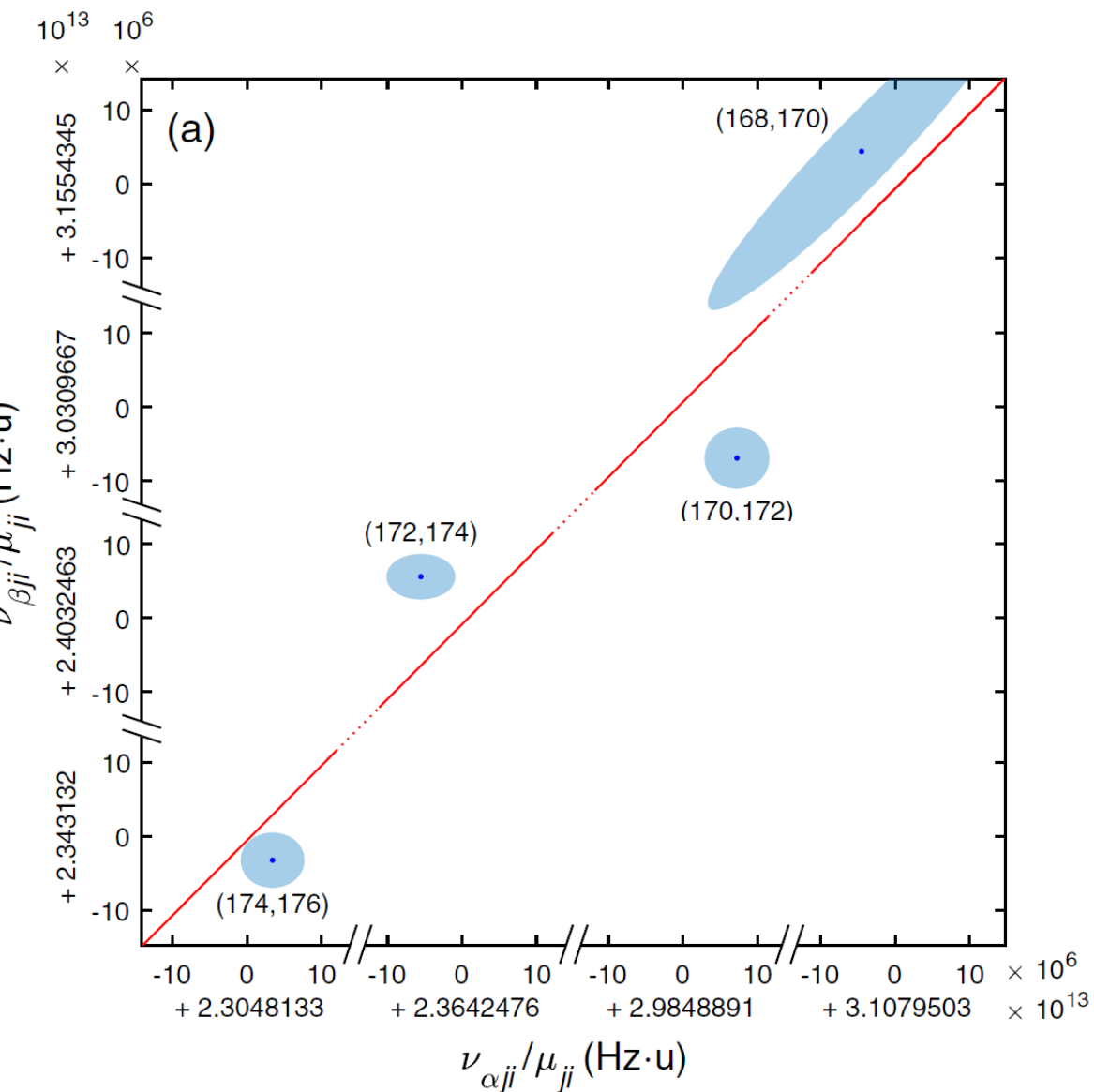
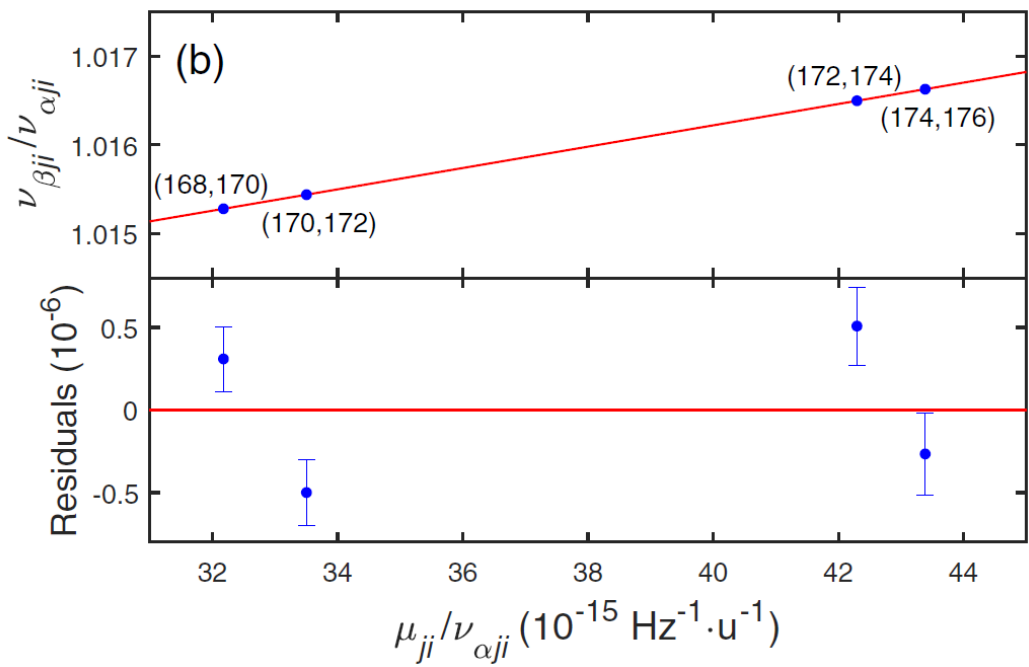
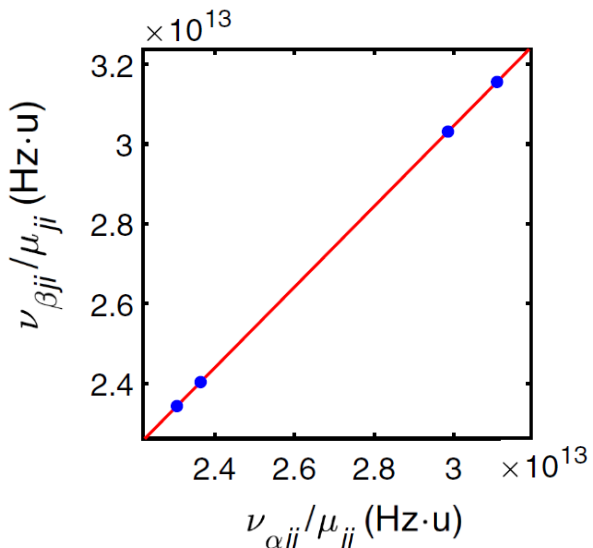
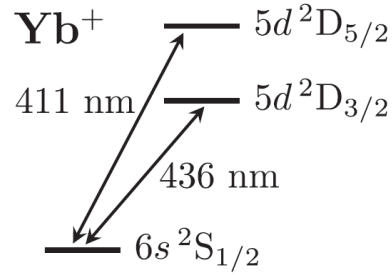


Phys. Rev. Lett. **115**, 053003 (2015)



Phys. Rev. Lett. **125**, 123003 (2020)

Isotope shift spectroscopy: Ytterbium



Phys. Rev. Lett. **125**, 123002 (2020)
+ more recent work at MIT, PTB, Mainz...

Isotope shift spectroscopy: Ytterbium

PHYSICAL REVIEW LETTERS 125, 123002 (2020)

Editors' Suggestion

Evidence of Two-Son-

Precision determination of isotope shifts in ytterbium and implications for new physics

N. L. Figueroa¹, J. C. Berengut², V. A. Dzuba², V. V. Flambaum², D. Budker¹, D. Antypas^{1,*}

¹ Johannes Gutenberg-Universität Mainz, Helmholtz-Institut Mainz,

GSI Helmholtzzentrum für Schwerionenforschung, 55128 Mainz, Germany

² School of Physics, University of New South Wales, Sydney, New South Wales 2052, Australia

(Dated: February 1, 2022)

We report measurements of isotope shifts for the five spinless Yb isotopes on the $6s^2 \ ^1S_0 \rightarrow 5d6s \ ^1D_2$ transition using Doppler-free two-photon spectroscopy. We combine these data with existing measurements on two transitions in Yb^+ [Phys. Rev. Lett. 125, 123002 (2020)], where deviation from King-plot linearity showed hints of a new bosonic force carrier at the 3σ level. The combined data strongly reduces the significance of the new-physics signal. We show that the observed nonlinearity in the joint Yb/Yb^+ King-plot analysis can be accounted for by the deformation of the Yb nuclei.

Isotope shift spectroscopy: Ytterbium

$$\tilde{v}_{\beta ji} = F_{\beta\alpha} \tilde{v}_{\alpha ji} + K_{\beta\alpha} + G_{\beta\alpha} (\delta \langle r^2 \rangle_{ji})^2 + v_{ne} D_{\beta\alpha} \tilde{a}_{ji}$$

+ $G'_{\beta\alpha} \delta \langle r^4 \rangle_{ji} + \dots$

quadrupole
deformations

field shift *mass shift* *second-order field shift* *New Boson*

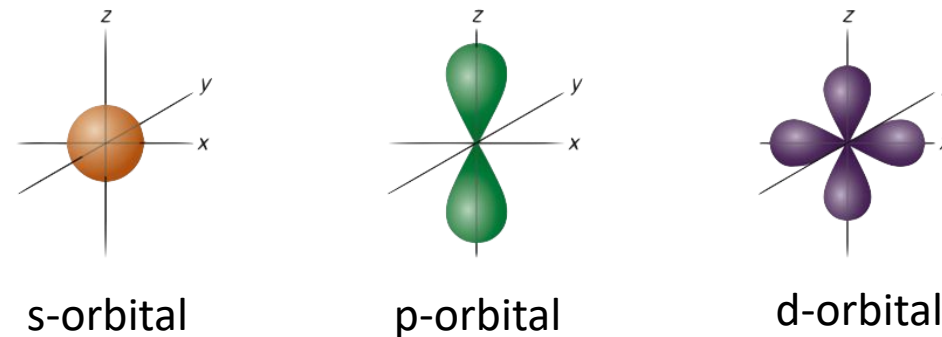
linear offset nonlinear / quadratic nonlinear



Isotope shift spectroscopy: Mercury

Now what?

- (1) Move away from s-orbitals



Suppression of field shift for non-s states in relativistic atoms:

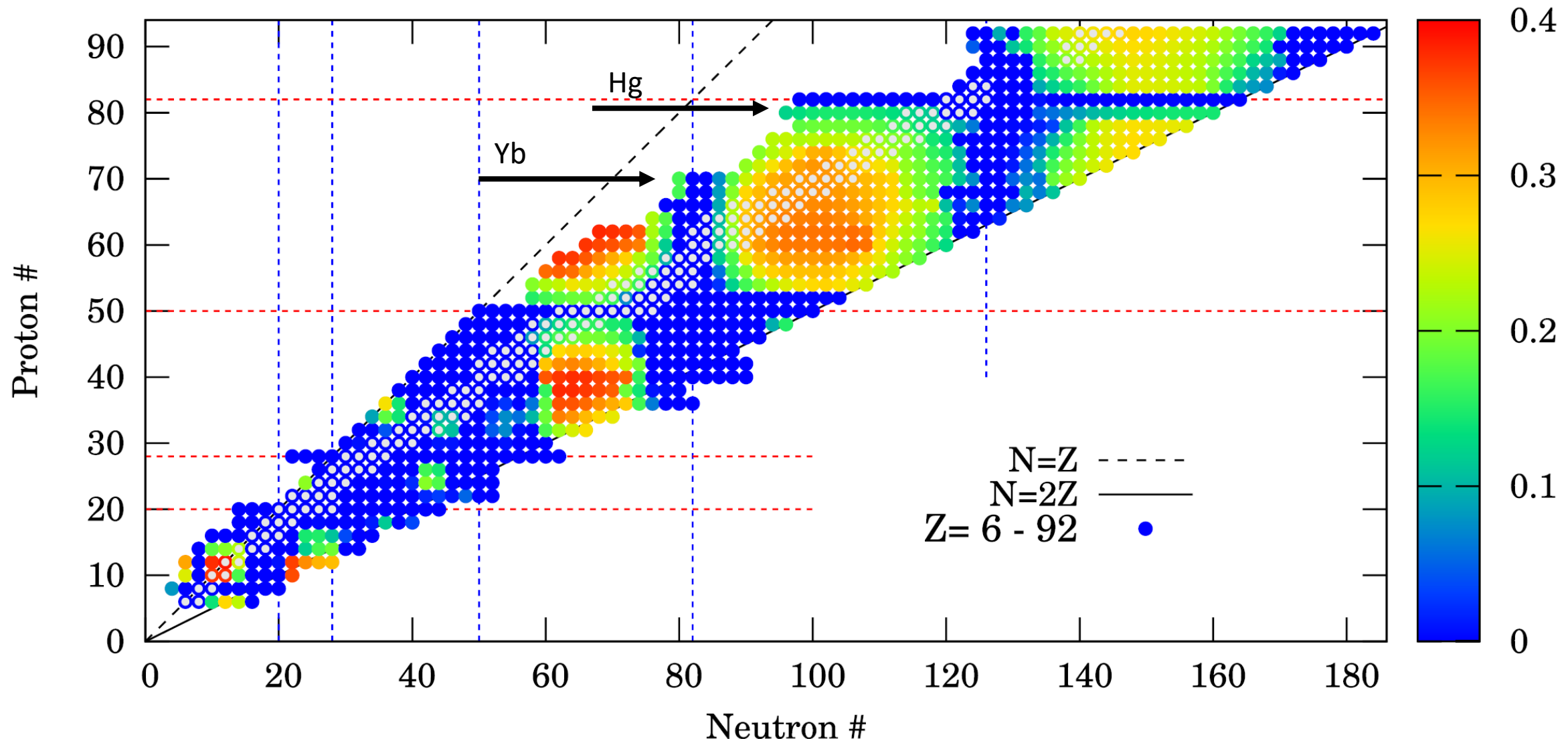
$$\frac{(Z\alpha)^2}{3} \approx \frac{1}{10} \quad \text{for mercury}$$

$$\frac{(Z\alpha)^2}{3} \approx \frac{1}{140} \quad \text{for calcium}$$

- (2) Search for nuclei with less quadrupole deformations

Isotope shift spectroscopy: Mercury

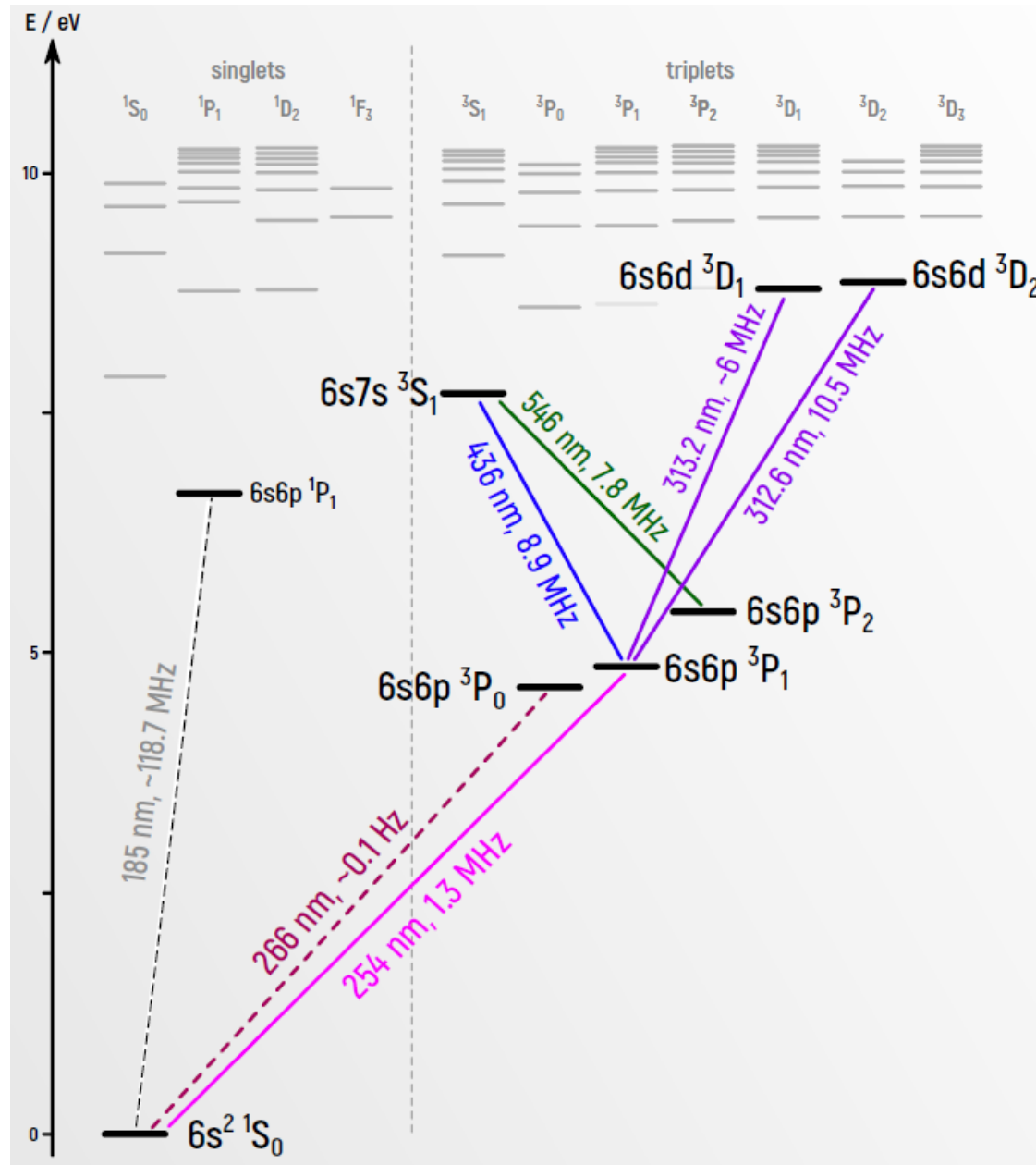
Quadrupole Deformation (# 1002)



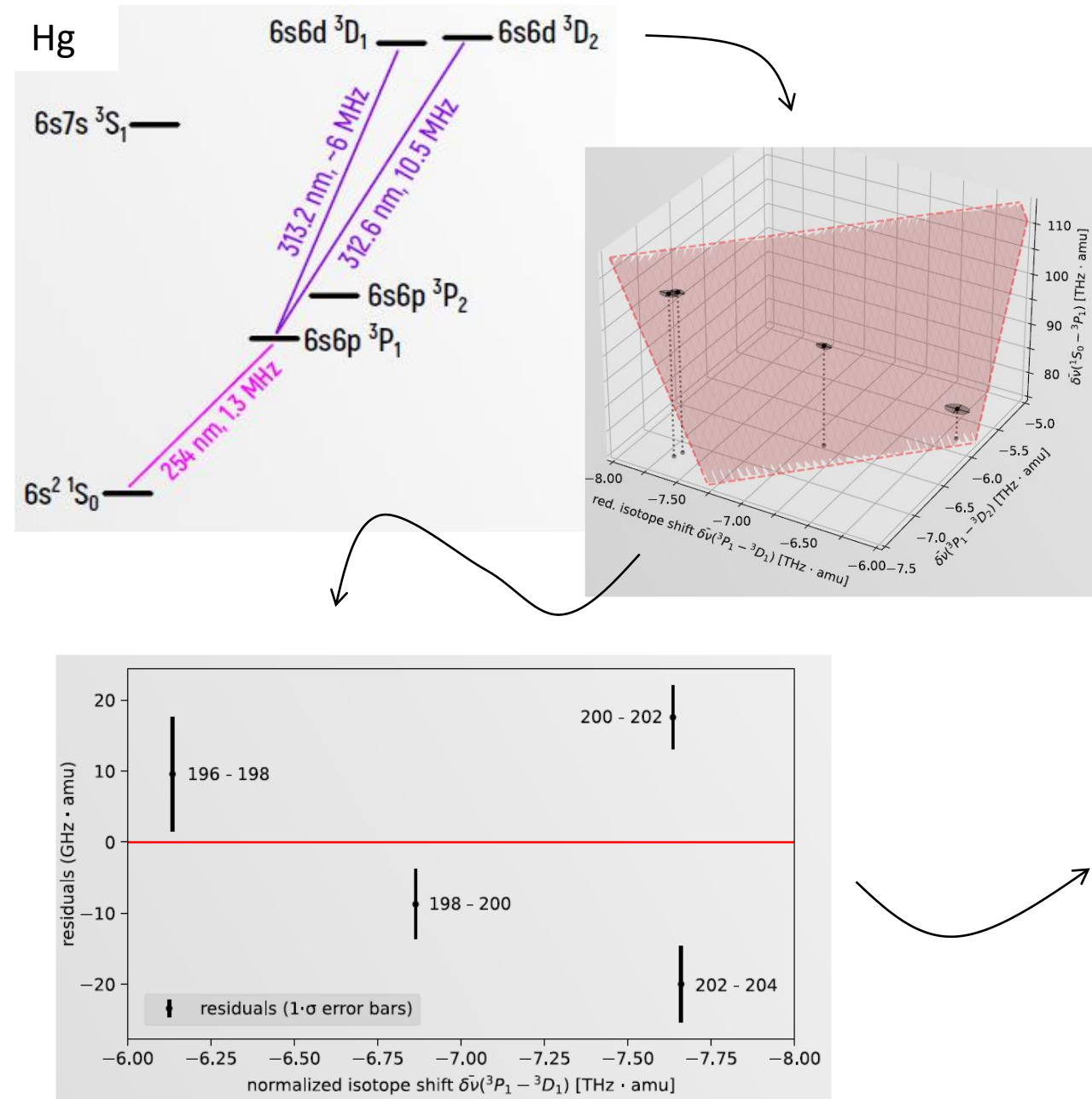
Isotope shift spectroscopy: Mercury

Mercury:

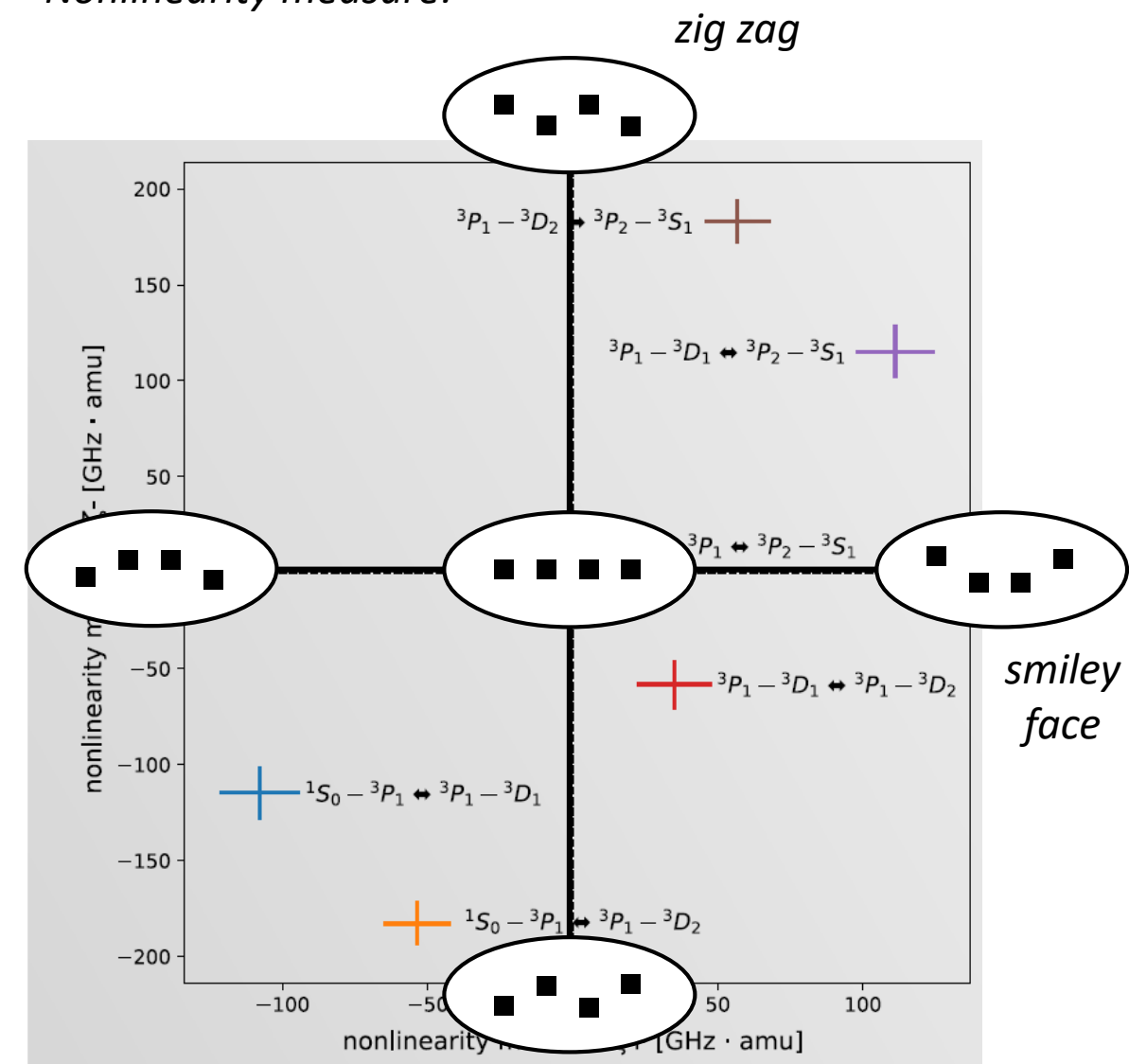
- 5 suitable isotopes
- Lots of transitions
- **Less quadrupole deformations than Yb**



Isotope shift spectroscopy: Mercury

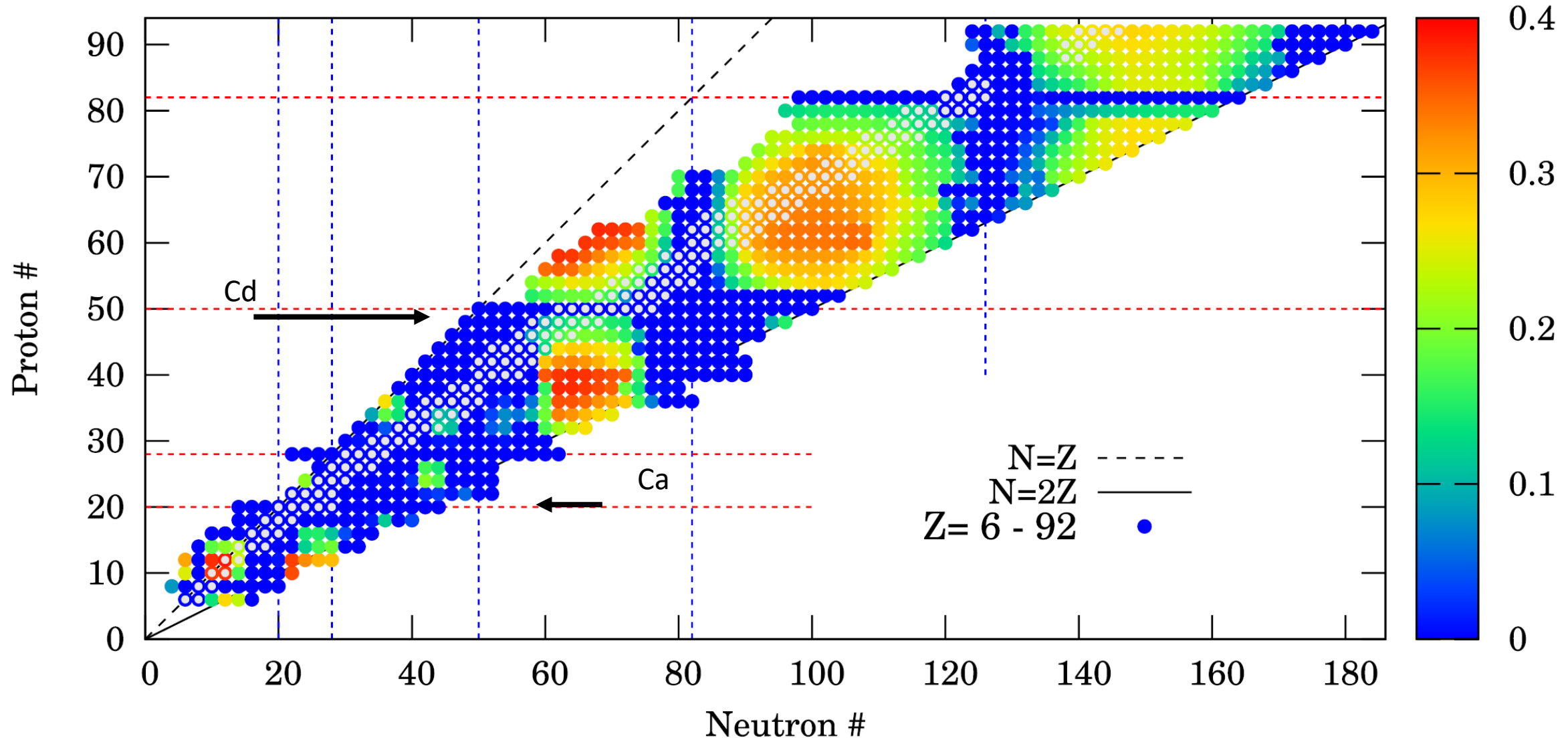


Nonlinearity measure:



Isotope shift spectroscopy

Quadrupole Deformation (# 1002)



Isotope shift spectroscopy: back to Calcium

Calcium:

- 5 stable bosonic isotopes
- nuclear shell closures at $N = 20$ and $N = 28$
- lots of very narrow transitions
- Compare with Ca^+ ions and HCl
- masses have been measured (last week!)

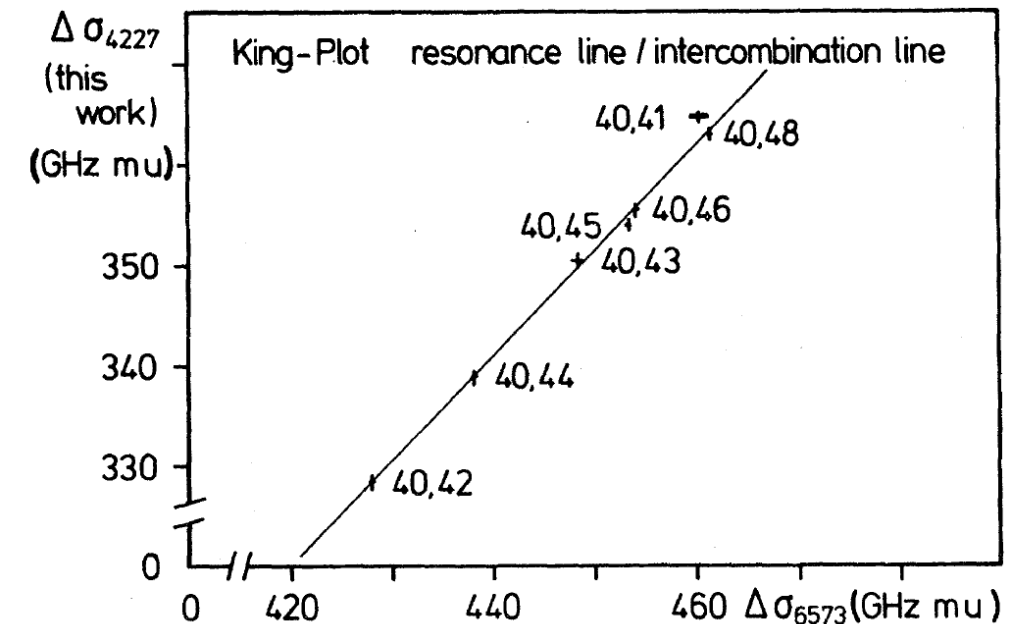
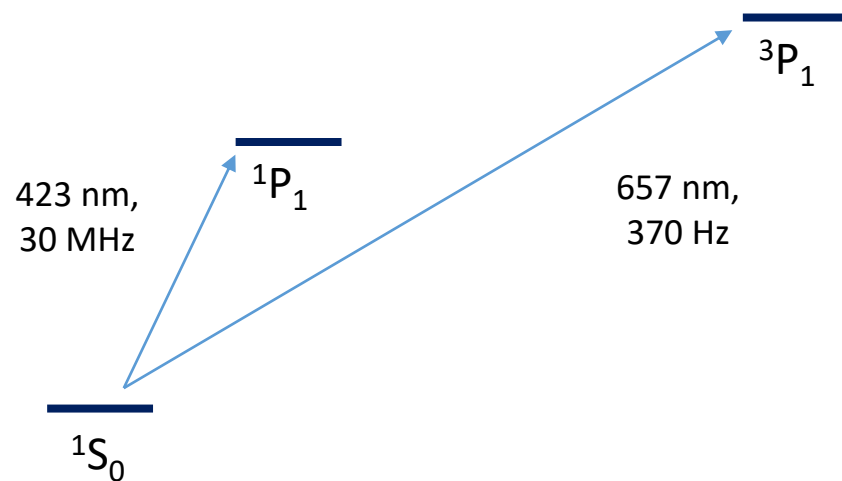
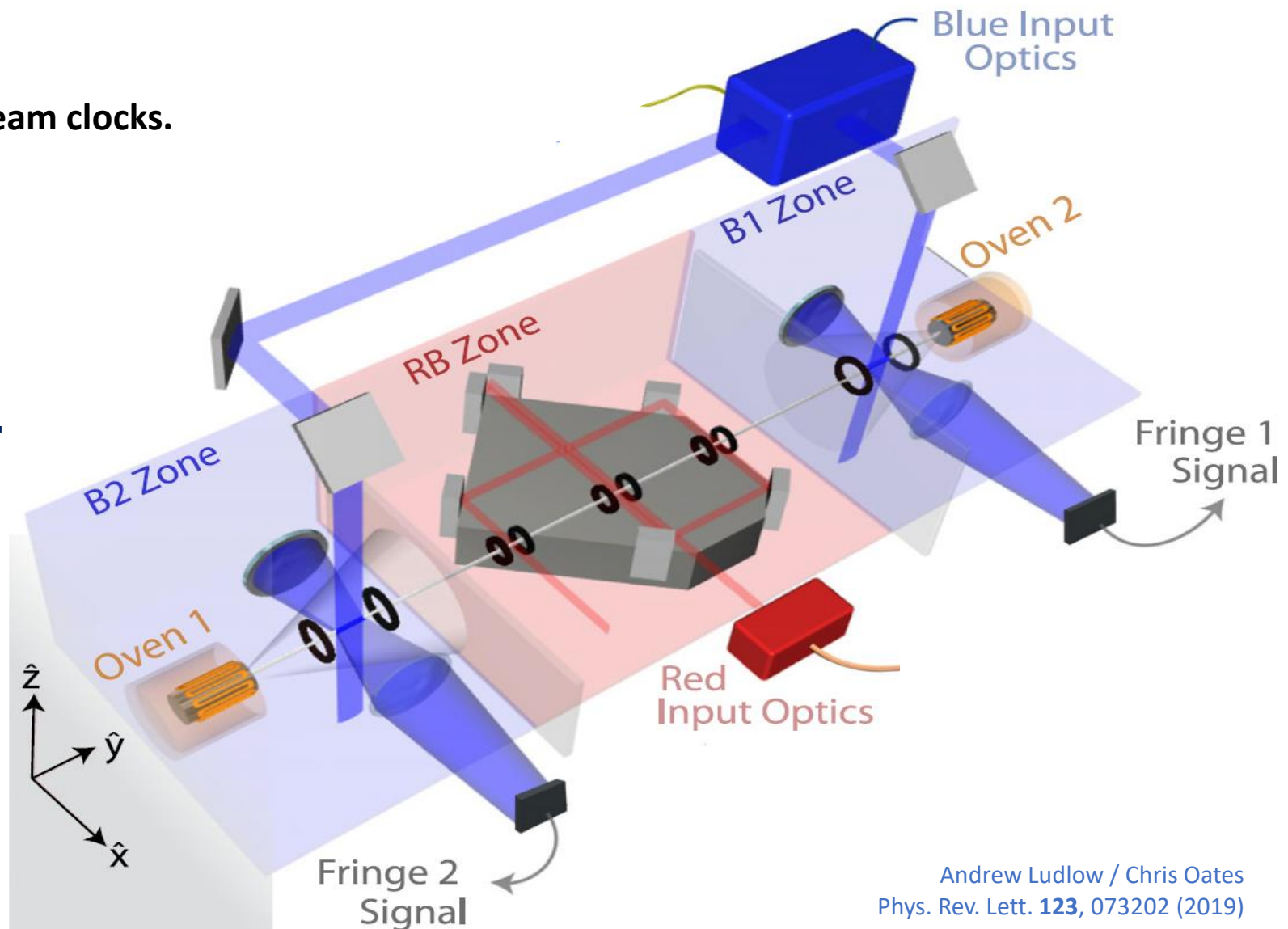
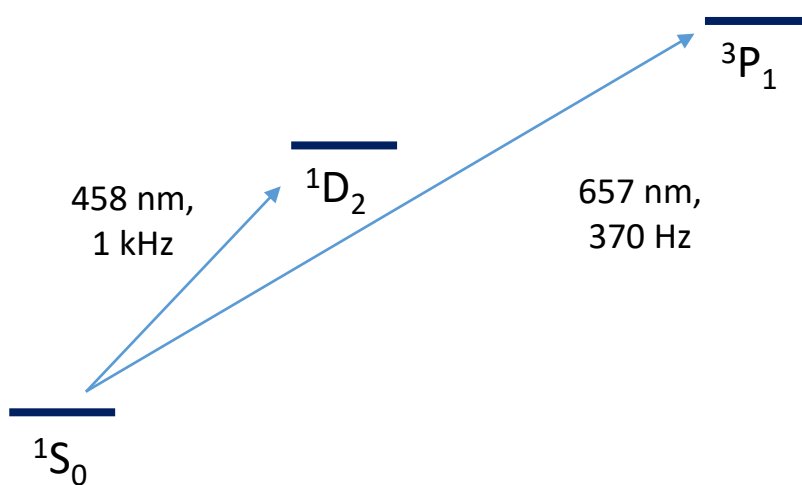


FIG. 2. King diagram with the isotope shifts of the CaI intercombination line $^1\text{S}_0 - ^3\text{P}_1$ ($\Delta\sigma = A'A / (A' - A) \times \delta\nu$).

Phys. Rev. C 26, 2194 (1982)

Isotope shift spectroscopy: back to Calcium

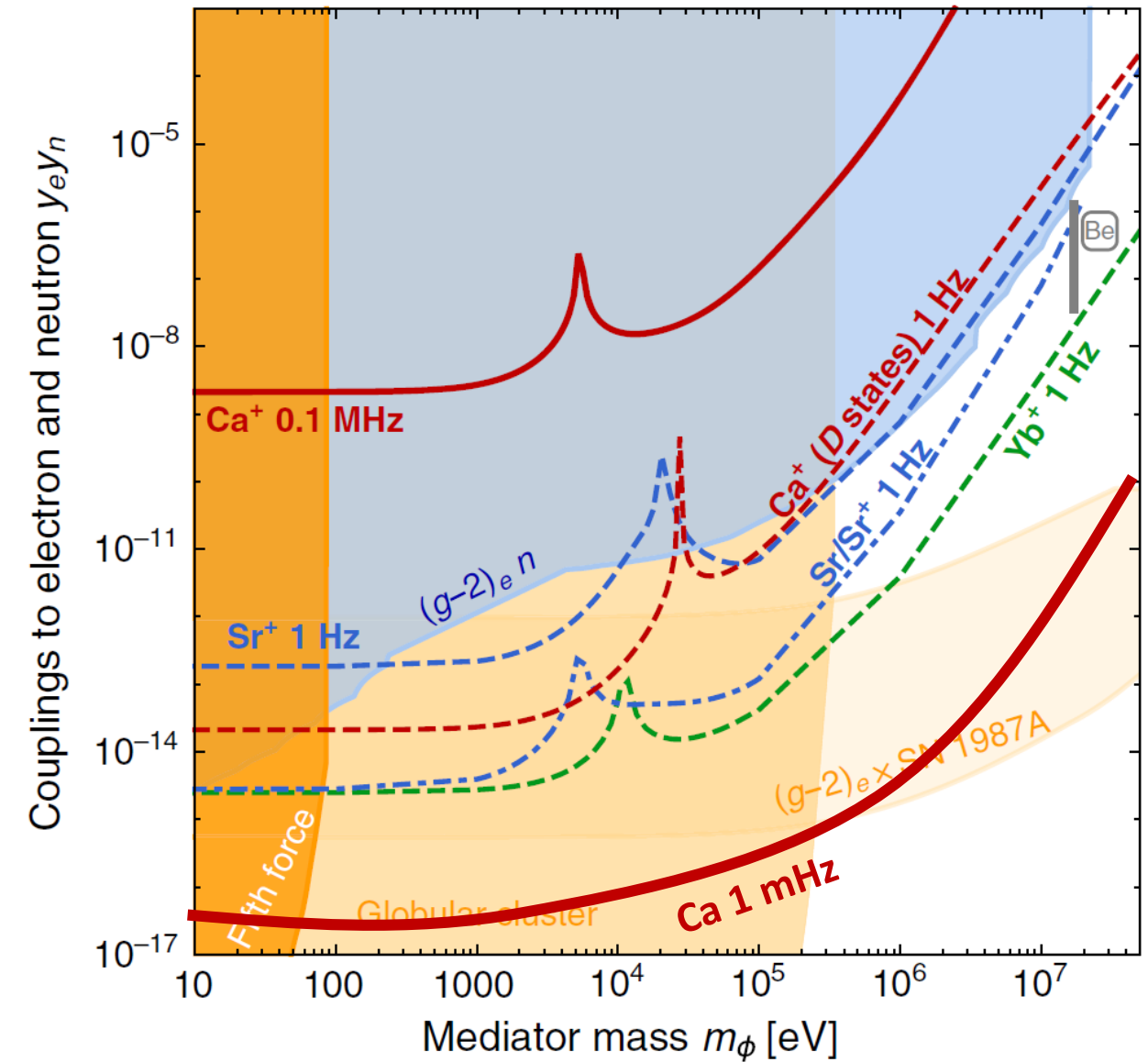
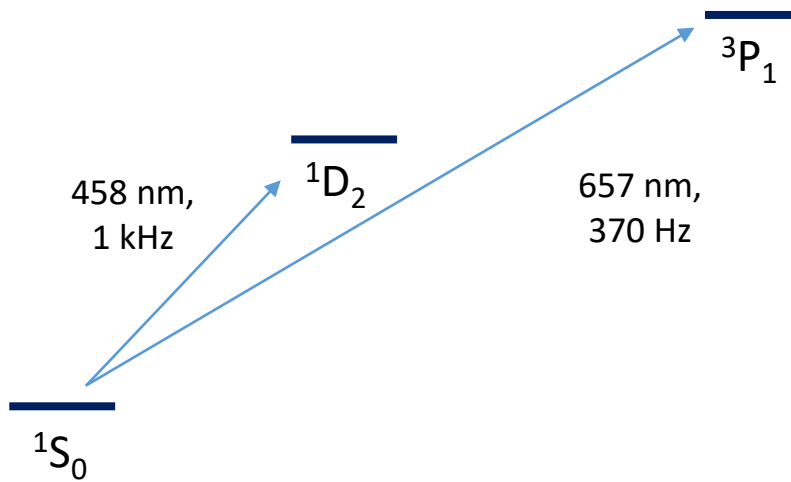
A new approach:
simultaneous operation of two calcium beam clocks.



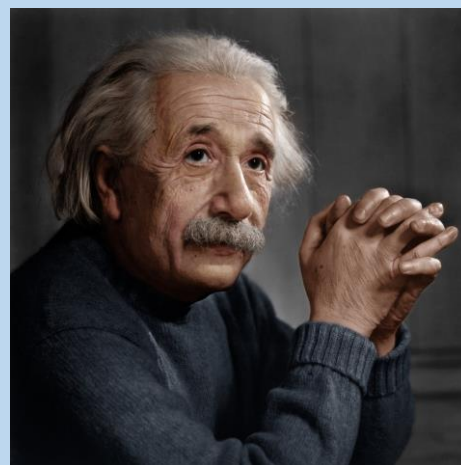
Isotope shift spectroscopy: back to Calcium

A new approach:
simultaneous operation of two calcium beam clocks.

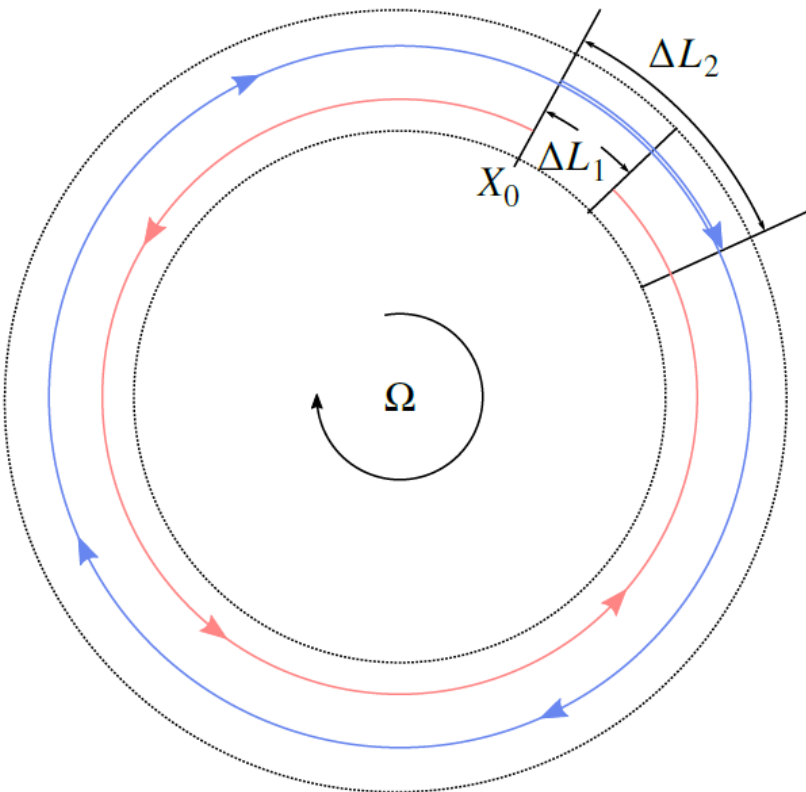
- target instability: 10^{-16}
- target sensitivity: mHz range



Test of special relativity



The Sagnac effect

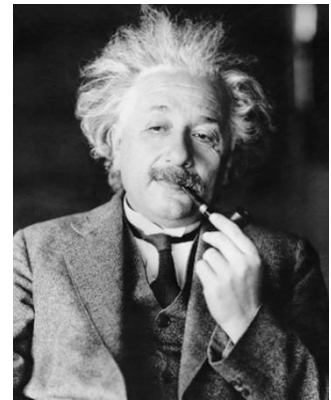


(1) For small rotation rates:

$$\begin{aligned}\Delta\tau &= \tau_1 - \tau_2 \\ &= \frac{4\pi R^2 \Omega}{c^2 - (\Omega R)^2} \\ &= \frac{4\pi R^2 \Omega}{c^2} \sum_{k=0}^{\infty} \left(\frac{\Omega R}{c}\right)^{2k} \\ &= \frac{4\pi R^2 \Omega}{c^2} \left(1 + \left(\frac{\Omega R}{c}\right)^2 + O\left(\left(\frac{\Omega R}{c}\right)^4\right)\right)\end{aligned}$$

$\Delta\tau = \frac{4A\Omega}{c^2}$

The Sagnac effect (1913)



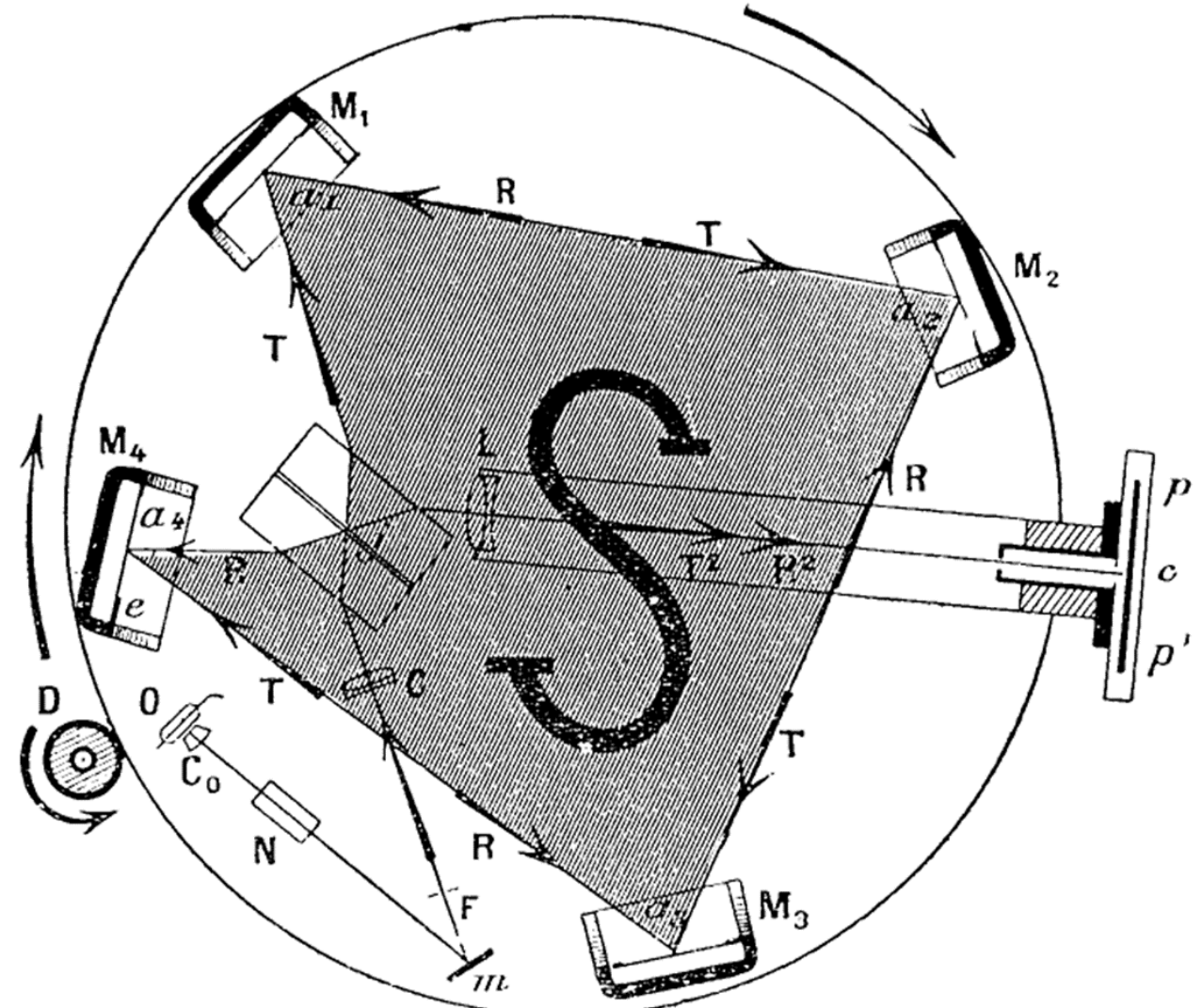
Albert Einstein



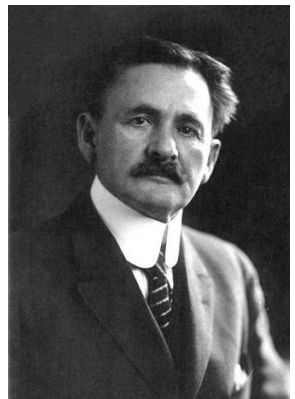
Max von Laue



George Sagnac



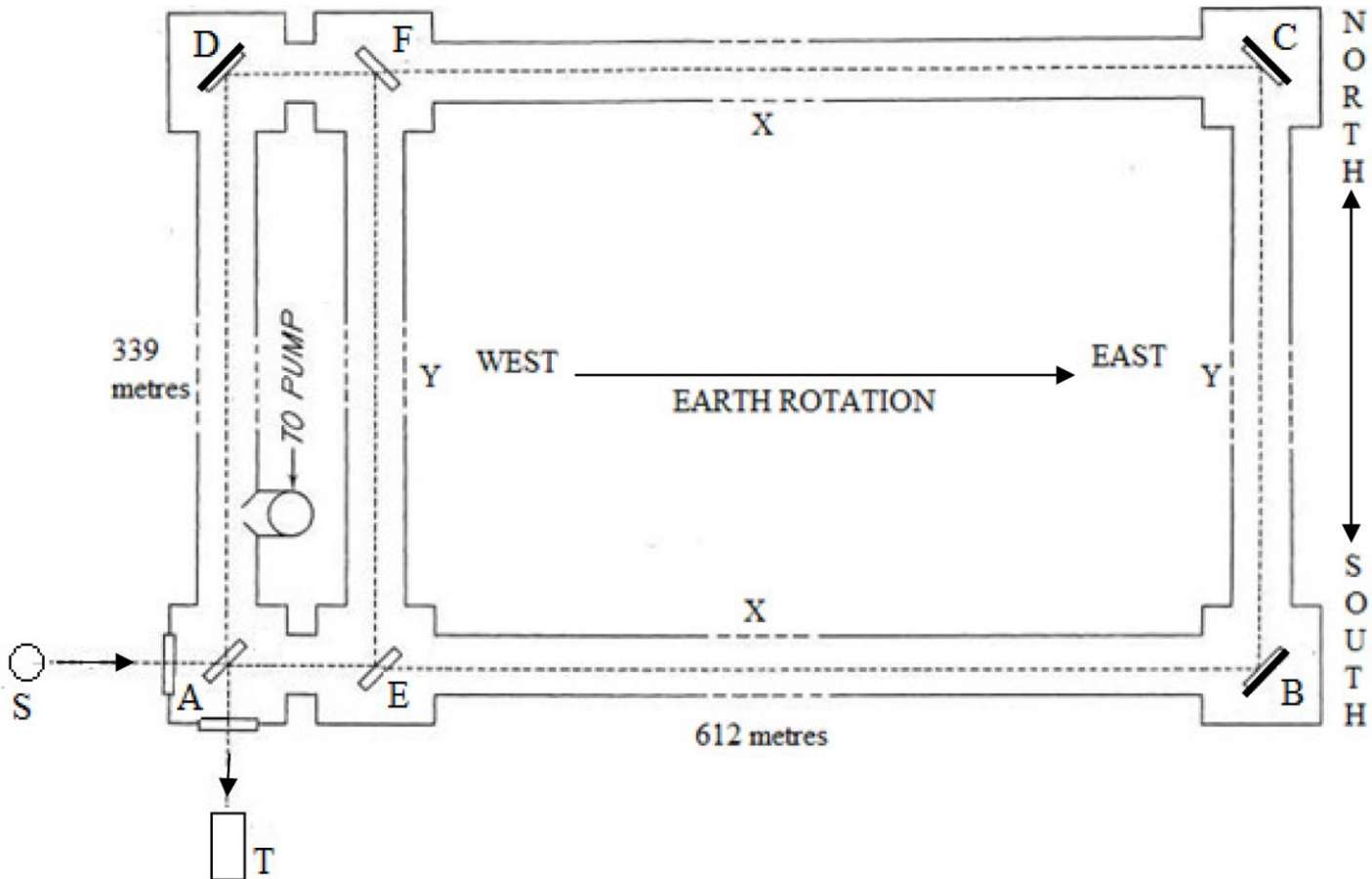
The Michelson-Gale experiment (1925)



Albert A. Michelson



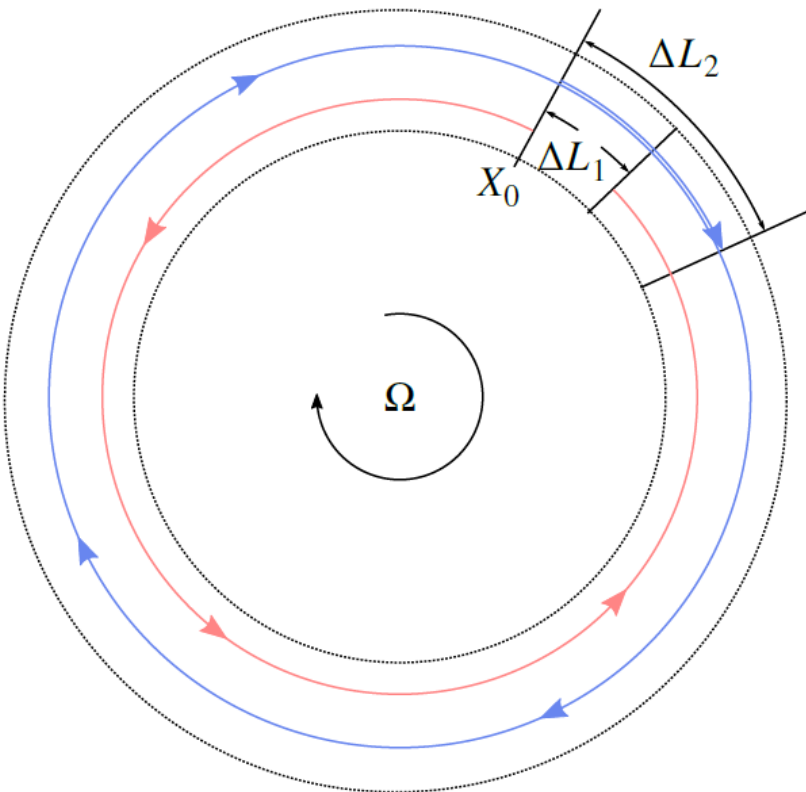
Henry G. Gale



calculated shift: 0.237 periods
measured shift: 0.230(5) periods

- > Earth is rotating! (*Cheers to Foucault (1851)!*)
- > First time that Sagnac is used for Earth rotation

The Sagnac effect



(2) From phase to frequency:

$$f_{Sagnac} = \frac{4}{\lambda S} \vec{A} \vec{\Omega}$$

(1) For small rotation rates:

$$\begin{aligned}\Delta\tau &= \tau_1 - \tau_2 \\ &= \frac{4\pi R^2 \Omega}{c^2 - (\Omega R)^2} \\ &= \frac{4\pi R^2 \Omega}{c^2} \sum_{k=0}^{\infty} \left(\frac{\Omega R}{c} \right)^{2k} \\ &= \frac{4\pi R^2 \Omega}{c^2} \left(1 + \left(\frac{\Omega R}{c} \right)^2 + O \left(\left(\frac{\Omega R}{c} \right)^4 \right) \right)\end{aligned}$$

$$\Delta\tau = \frac{4}{c^2} \vec{A} \vec{\Omega}$$

(3) Consider a square of arm length L :

$$f_{Sagnac} = \frac{L}{\lambda} \Omega \sin \theta$$

„scale factor“ $\in \mathbb{N}, \mathcal{O}(10^7)$

The Sagnac effect

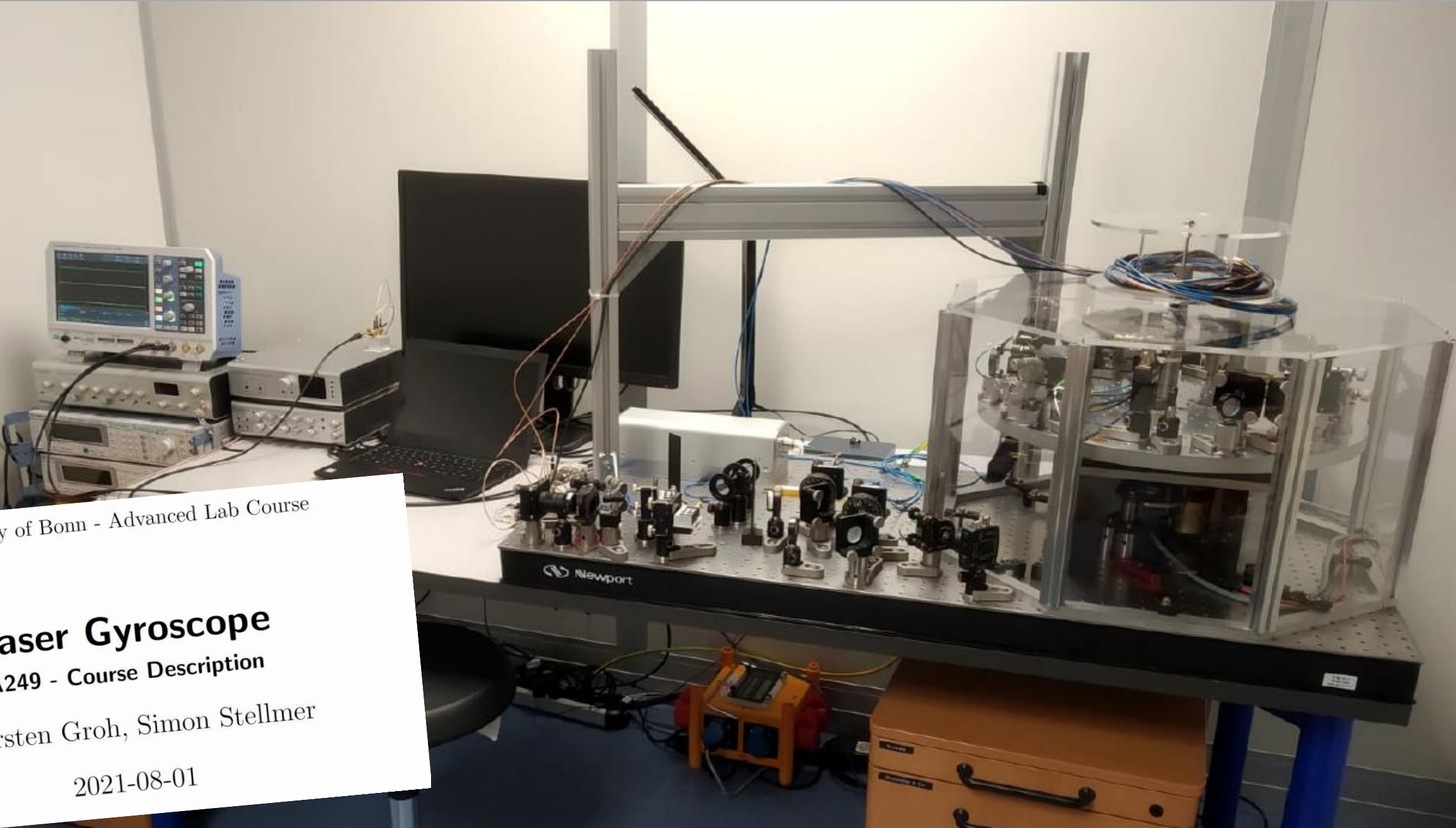
University of Bonn - Advanced Lab Course

Laser Gyroscope

A249 - Course Description

Thorsten Groh, Simon Stellmer

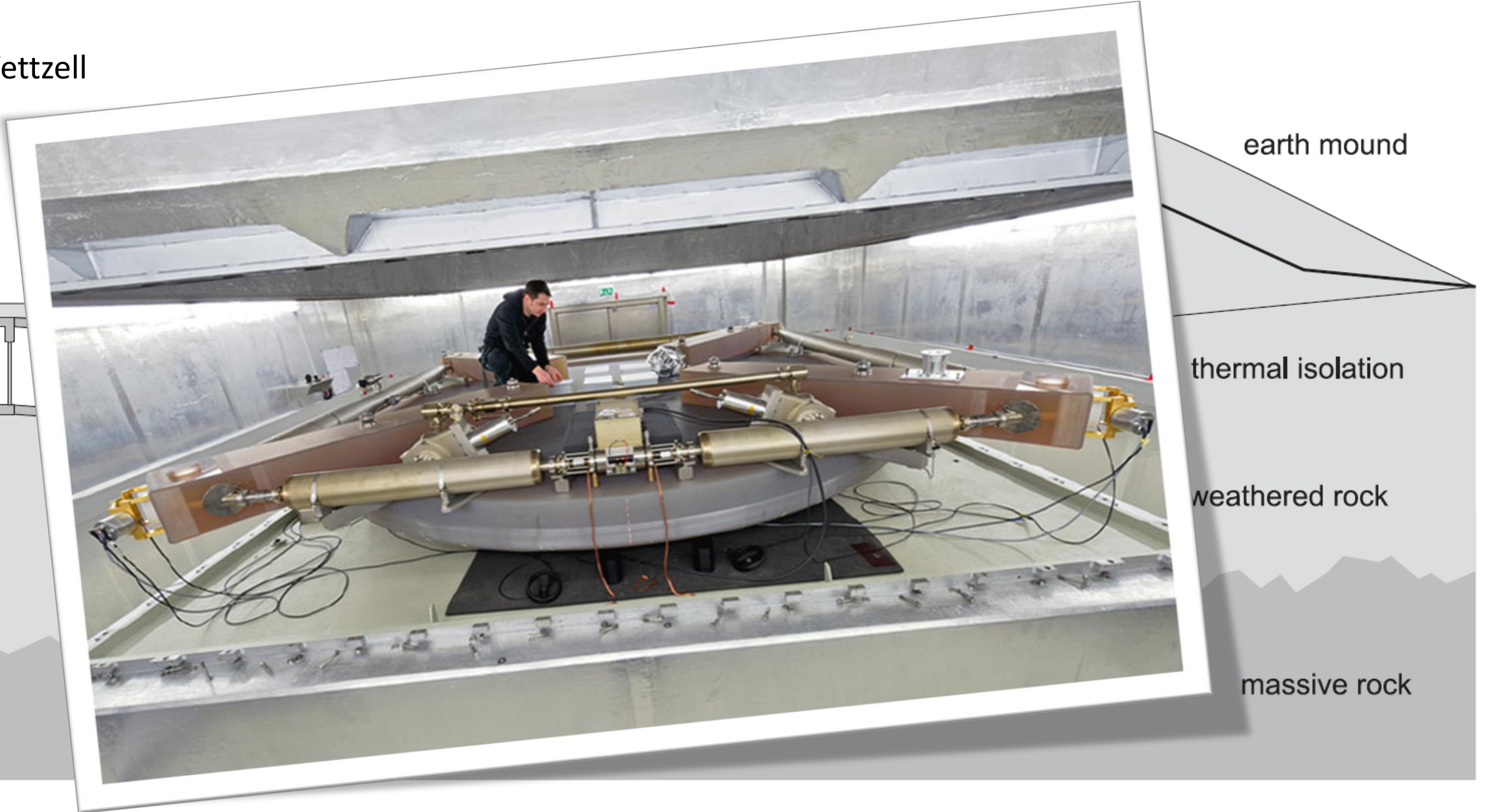
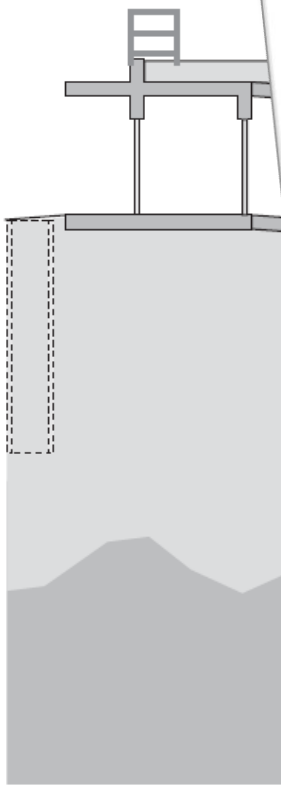
2021-08-01





The G Ring at Wettzell

G ring, Wettzell



earth mound

thermal isolation

weathered rock

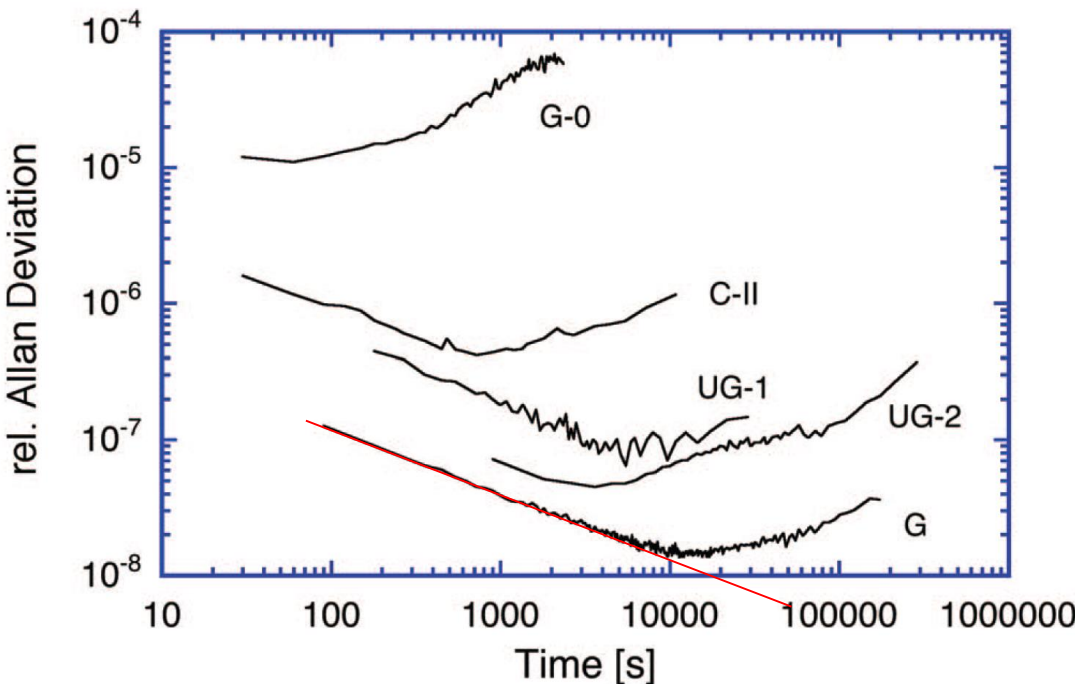
massive rock

The G Ring at Wettzell

Sensitivity:

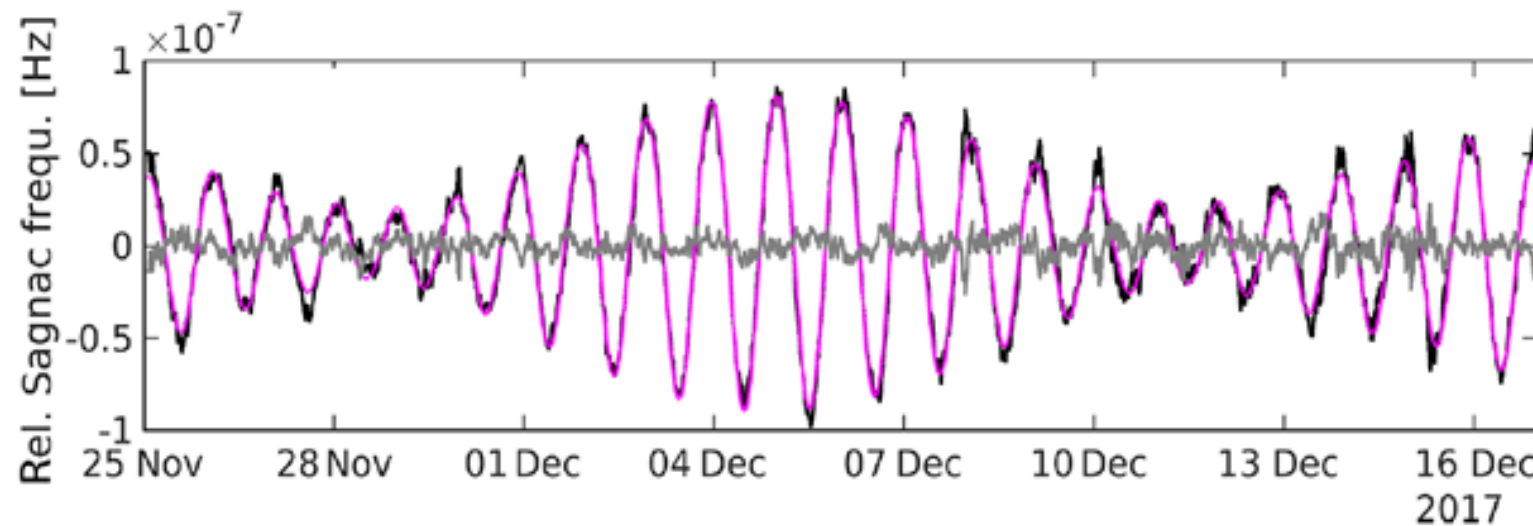
$$\delta\Omega = \frac{1}{4} \frac{c\lambda}{L^2 F} \sqrt{\frac{h\nu}{P}} \frac{1}{\tau}$$

G ring (Wettzell): $\delta\Omega = 12 \text{ prad/s}/\sqrt{\text{Hz}}$



Take-home message:
 10^{-8} within 3 hours

Earth rotation...
tidal effects !



sub-diurnal
variations !

Test of special relativity

$$f_{Sagnac} = \frac{L}{\lambda} \Omega_E \sin \theta$$

Test of special relativity

Sagnac frequency:

Our observable, at the 10^{-9} level

$$f_{Sagnac} = \frac{L}{\lambda} \Omega_E \sin \theta$$

Test of special relativity

Sagnac frequency:

Our observable, at the 10^{-9} level

Earth rotation rate

$$f_{Sagnac} = \frac{L}{\lambda} \Omega_E \sin \theta$$

IERS: International Earth Rotation Service (= astronomy)

The contributed observations used in the preparation of this Bulletin are available at <<http://www.usno.navy.mil/USNO/earth-orientation/eo-info/general/input-data>>. The contributed analysis results are based on data from Very Long Baseline Interferometry (VLBI), Satellite Laser Ranging (SLR), the Global Positioning System (GPS) satellites, Lunar Laser Ranging (LLR), and meteorological predictions of variations in Atmospheric Angular Momentum (AAM).

COMBINED EARTH ORIENTATION PARAMETERS:

IERS Rapid Service							
MJD	x "	error "	y "	error "	UT1-UTC s	error s	
22 10 14	59866	0.25701	.00009	0.23208	.00009	-0.005444	0.000014
22 10 15	59867	0.25408	.00009	0.23040	.00009	-0.005177	0.000013
22 10 16	59868	0.25116	.00009	0.22886	.00009	-0.004895	0.000014
22 10 17	59869	0.24810	.00009	0.22721	.00009	-0.004671	0.000016
22 10 18	59870	0.24528	.00009	0.22512	.00009	-0.004559	0.000016
22 10 19	59871	0.24299	.00009	0.22296	.00009	-0.004593	0.000017
22 10 20	59872	0.24079	.00009	0.22122	.00009	-0.004790	0.000019

Last week

Error on pole coordinates:
0.09 mas = 2.7 mm

Error in length-of-day: ~ 10 µs

10 µs / 24 hours
= 10^{-12}

Test of special relativity

Sagnac frequency:
our observable, at the 10^{-9} level

Earth rotation rate:
from VLBI, at the 10^{-12} level

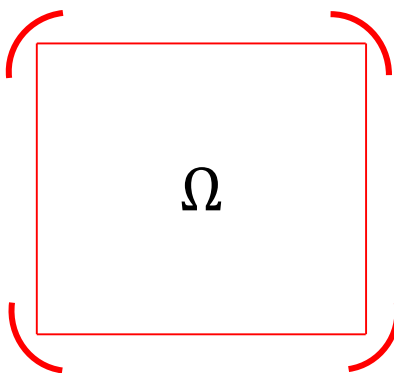
$$f_{Sagnac} = \frac{L}{\lambda} \Omega_E \sin \theta$$

Scale factor

Test of special relativity

longitudinal mode
number N

$$\frac{L}{2\lambda} \cong N = \frac{f}{FSR}$$



Measured with a frequency comb:

$$f = 473\,612\,701.08 \pm 0.15 \text{ MHz}$$

$$FSR = 18.734\,385\,26 \pm 2 \text{ MHz}$$

$$\rightarrow N = 25\,280\,397.23 \pm 0.28$$

$$\rightarrow P = 16.002\,252\,12 \text{ m}$$

Test of special relativity

Sagnac frequency:
our observable, at the 10^{-9} level

Earth rotation rate:
from VLBI, at the 10^{-12} level

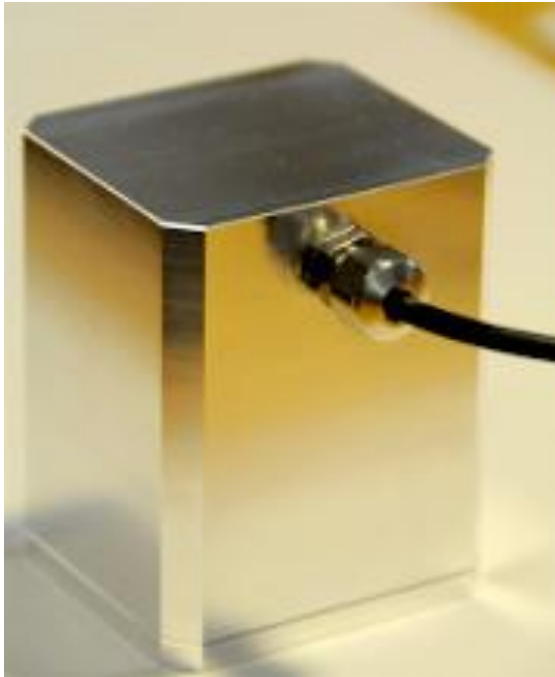
$$f_{Sagnac} = \frac{L}{\lambda} \Omega_E \sin \theta$$

Scale factor:
integer number (25 280 397)

Projection onto rotation axis

Test of special relativity

- (1) Use IERS data to fix pole coordinates to within 0.1 mas (3×10^{-10})
- (2) Use on-site VLBI, LL, SLR, GNSS etc. to determine G ring position (= latitude θ) to better than 10 cm (1×10^{-8})
- (3) Use tiltmeters to level the ring laser at sub-nrad precision ($< 10^{-9}$)



Tiltmeter



Space-geodetic techniques

Test of special relativity

Sagnac frequency:
our observable, at the 10^{-9} level

Earth rotation rate:
from VLBI, at the 10^{-12} level

$$f_{Sagnac} = \frac{L}{\lambda} \Omega_E \sin \theta$$

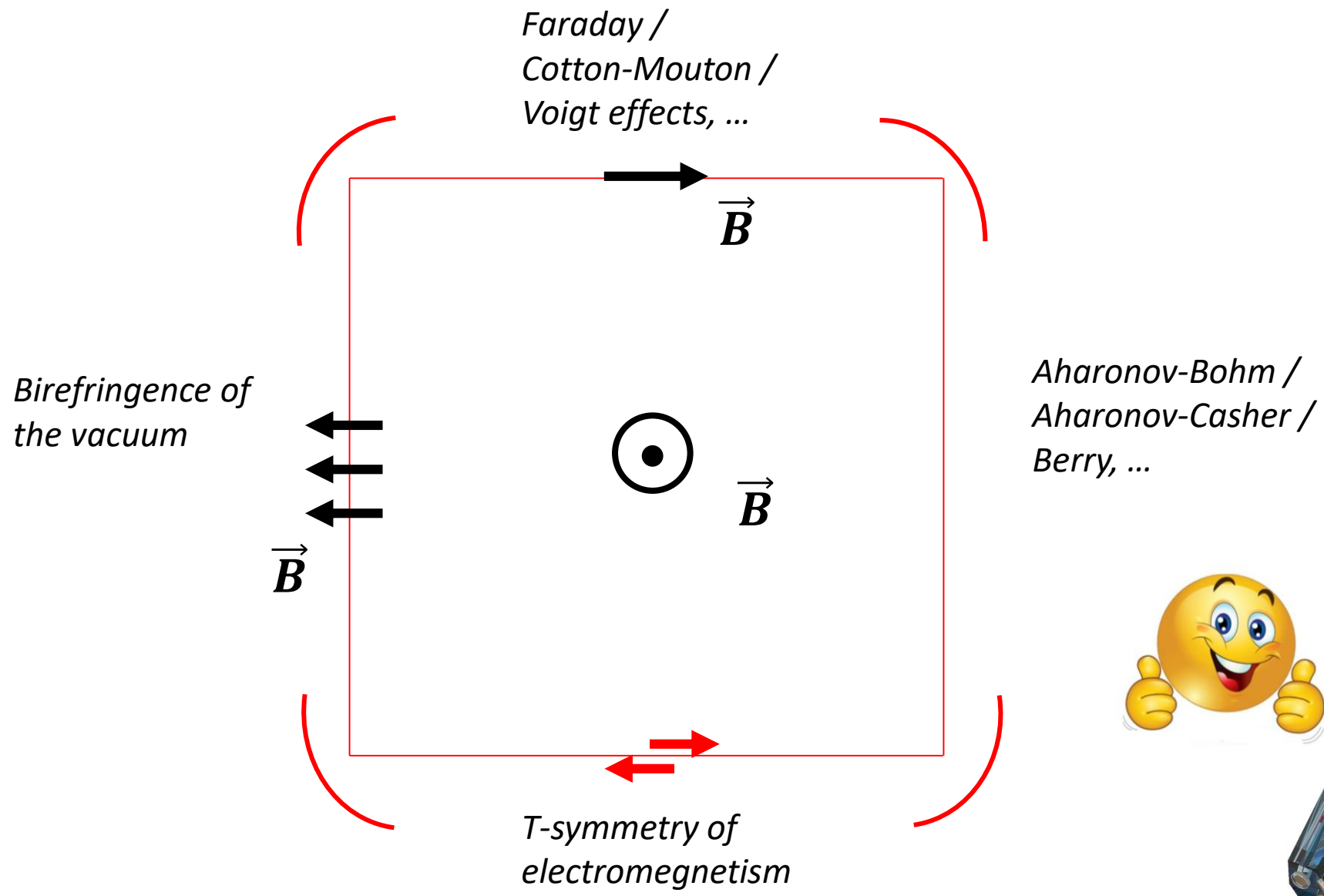
Scale factor:
integer number (25 280 397)

Projection onto rotation axis:
 10^{-8} to 10^{-9} level

The GeoSensor

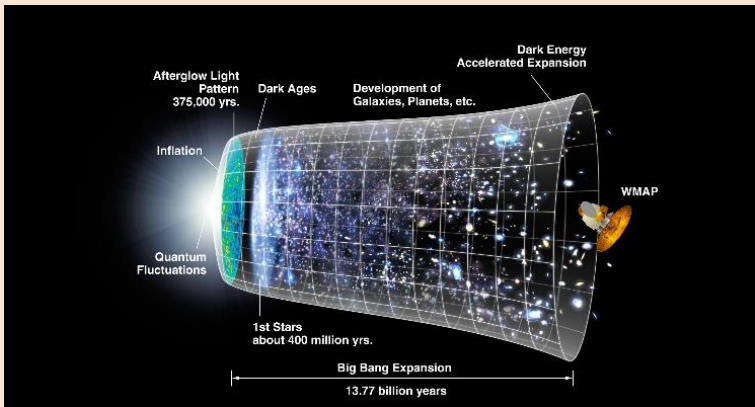


Magneto optics

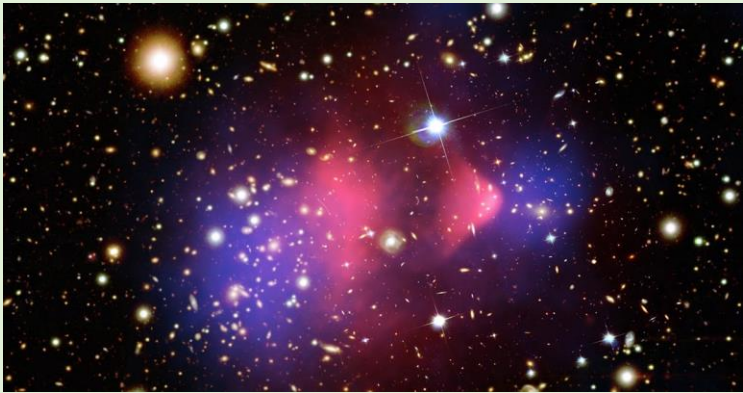


Grand challenges in fundamental physics

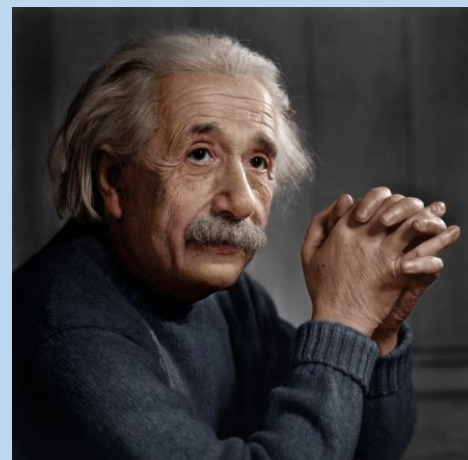
Baryon asymmetry



New particles



Test of special relativity



PhDs

Thorsten Groh
Quentin Lavigne
David Röser
Alireza Aghababaei
Stefan Schröder
Jannik Zenner
Anica Hamer

Thanks to a great team



Master students

Lukas Möller
Felix Affeld
Marc Vöhringer
Lara Becker

